SAND81-0938
UNLIMITED RELEASE

CATEGORY UC-92A

B6445

D1.2946

THE FORMATION INTERFACE FRACTURING EXPERIMENT: AN IN SITU INVESTIGATION OF HYDRAULIC FRACTURE BEHAVIOR NEAR A MATERIAL PROPERTY INTERFACE

MASTER

N. R. WARPINSKI, D. A. NORTHROP, R. A. SCHMIDT,
W. C. VOLLENDORF, AND S. J. FINLEY

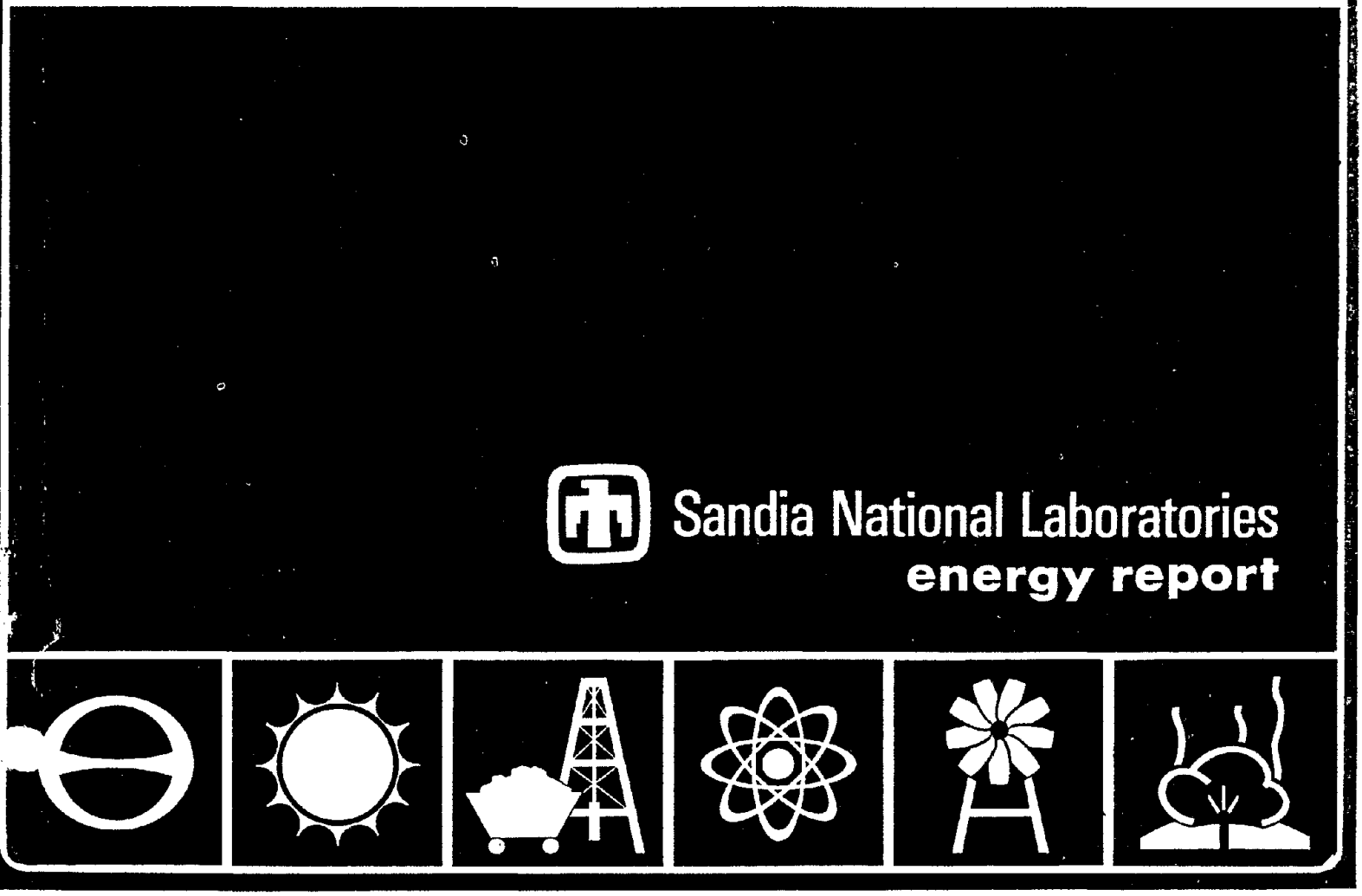

SF 2900-QQB(3-80)
DISTRIBUTION OF THIS DOCUMENT IS UNLIMITED

Issued by Sandia Laboratories, operated for the United States Department of Energy by Sandia Corporation.

NOTICE

This report was prepared as an account of work sponsored by the United States Government. Neither the United States nor the Department of Energy, nor any of their employees, nor any of their contractors, subcontractors, or their employees, makes any warranty, express or implied, or assumes any legal liability or responsibility for the accuracy, completeness or usefulness of any information, apparatus, product or process disclosed, or represents that its use would not infringe privately owned rights.

Printed in the United States of America

Available from
National Technical Information Service
U. S. Depatment of Commerce
5285 Port Royal Road
Springfield, VA 22161

Price: Printed Copy $6.00, Microfiche $3.00

DISCLAIMER

Portions of this document may be illegible in electronic image products. Images are produced from the best available original document.

DISCLAIMER

This book was prepared as an account of work sponsored by an agency of the United States Government. Neither the United States Government nor any agency thereof, nor any of their employees, makes any warranty, express or implied, or assumes any legal liability or responsibility for the accuracy, completeness, or usefulness of any information, apparatus, product, or process disclosed, or represents that its use would not infringe privately owned rights. Reference herein to any specific commercial product, process, or service by trade name, trademark, manufacturer, or otherwise, does not necessarily constitute or imply its endorsement, recommendation, or favoring by the United States Government or any agency thereof. The views and opinions of authors expressed herein do not necessarily state or reflect those of the United States Government or any agency thereof.

SAND81-0938

Unlimited Release

The Formation Interface Fracturing Experiment: An In Situ Investigation of Hydraulic Fracture Behavior Near a Material Property Interface

Final Report

N. R. Warpinski, D. A. Northrop, R. A. Schmidt,
W. C. Vollendorf and S. J. Finley

ABSTRACT

Hydraulic fracture experiments have been conducted to examine fracture behavior at a formation interface. These experiments are being conducted near an existing tunnel complex and mineback through the region allows for the direct observation and characterization of the fracture system. Two hydraulic fractures were created, one above and one below an ash-fall tuff - welded tuff formation interface. These formations, respectively, have significant differences in their Young's moduli (0.5×10^6, 5.0×10^6 psi), Poisson's ratios (0.30, 0.21) and porosities (45, 13%). Sufficient cement was injected into each zone to create vertical fractures of 600 ft total length if the height was restricted to 50 ft; 256 and 117 bbls were injected at 6 bbls/min into the ash-fall tuff and welded tuff zones, respectively.

Mineback along the interface has revealed a total fracture length of 150 ft; coring has shown that the heights of the fractures are about 100 ft for the fracture initiated in the ash-fall tuff and 200 ft for the welded tuff fracture. The fracture which was initiated in the low modulus ash-fall tuff propagated upwards into the higher modulus welded tuff. No containment was observed. The results from the fracture subsequently initiated in the welded tuff are obscured because it propagated alongside the lower fracture and thus provided no definitive information on behavior at the interface. Widths in both the ash-fall

DISTRIBUTION OF THIS DOCUMENT IS UNLIMITED

and welded tuffs are consistent with design calculations. The in situ stresses were found to have the greatest effect on fracture behavior and geometry. Variations in the minimum principal in situ stress controlled the direction of fracture propagation and the final height of the fracture. The low stress measured in the welded tuff probably aided the propagation of the fracture into that region. Natural fractures in the welded tuff caused significant offsets in the induced fractures and resulted in filling of some of the natural fractures with grout and severe fluid leakoff.

These experiments show that material property interfaces should not, in general, be considered containment features. A more likely factor in controlling fracture height is in situ stress differences.

TABLE OF CONTENTS

INTRODUCTION

The frequent failure of stimulation techniques such as massive hydraulic, dendritic, foam, gas, and chemical explosive fracturing has usually been attributed to either inadequate reservoir characterization or unfavorable and unexpected fracture behavior. The latter result includes many different possible phenomena, none of which are readily observed from the well bore. In situ examination of hydraulic fractures through mineback techniques, however, offers an ideal method of conducting fracture research and observing firsthand the effects of faults, fractures, geologic interfaces, and variations in in situ stresses, elastic moduli, and other important parameters. Such observations, together with complete pumping schedules, pressure records, geologic structure, material properties and in situ stress measurements, should be sufficient to characterize the fracture, compare the end result with that predicted by models and hopefully offer insight into the phenomena of fracture propagation.

Mineback experiments are controlled in situ evaluations of hydraulic, explosive and other stimulation techniques by physical mining of the rock mass in the vicinity of the test area and direct observation of the results. These tests are presently being conducted using existing tunnel facilities and mining capabilities at the Nevada Test Site, Nye County, Nevada. Fractures, which are created in Rainier Mesa under 1200 - 1400 ft of overburden, are mined back with a rotating drum mining machine which provides a clean face cut for easy fracture identification. A detailed physical description can be obtained directly by observation and documented with photography and field mapping and can be correlated with important geophysical parameters. Supportive rock and fluid mechanics laboratory and modeling work must be performed to aid in the interpretation. The mineback also provides the opportunity for the calibration of instrumentation techniques under known conditions.

Thus, mineback testing provides significantly more information than the evaluation of a commercial stimulation which is based primarily upon gas production.

The location of previous experiments is indicated in Figure 1, which shows the geophysical experiment area of G tunnel. The Hole #3 experiment[1] was a mineback of two grout-filled fractures that were propagated in ash-fall tuff from two separate zones at different depths in the same hole. The Hole #5 experiment[2,3] was an examination of the extremely complex fracture behavior observed in a region of abundant natural fractures, faults and bedding planes. Puff 'n Tuff[4] was a study of the rock mass behavior induced by the release of post-detonation high pressure gases from a spherical, high-explosive charge.

The Formation Interface Fracture Experiment is an examination of the behavior of hydraulic fractures at a geologic formation interface. Fractures were created both above and below a geologic formation interface consisting of a welded volcanic ash flow tuff underlain by a much lower modulus bedded ash-fall tuff. Mineback of these fractures provided direct observation of fracture behavior at the interface. Previous reports have detailed the geology, rock properties, fracture design and treatment operations[5] and the initial mineback results.[6] This report contains the final mineback results, results of an exploratory coring program to locate the extremities of the fracture, in situ stress data and a final analysis of the experiment.

FRACTURE BEHAVIOR AT A FORMATION INTERFACE

A hydraulic fracture is usually designed to be contained within the pay zone where it was initiated. Failure to do this results in an effective loss of the expensive fluid and proppant used to fracture the unproductive strata or other deleterious effects should the fracture penetrate a water-bearing zone. Present design calculations assume that the hydraulic fracture is bounded and this results in a vertical,

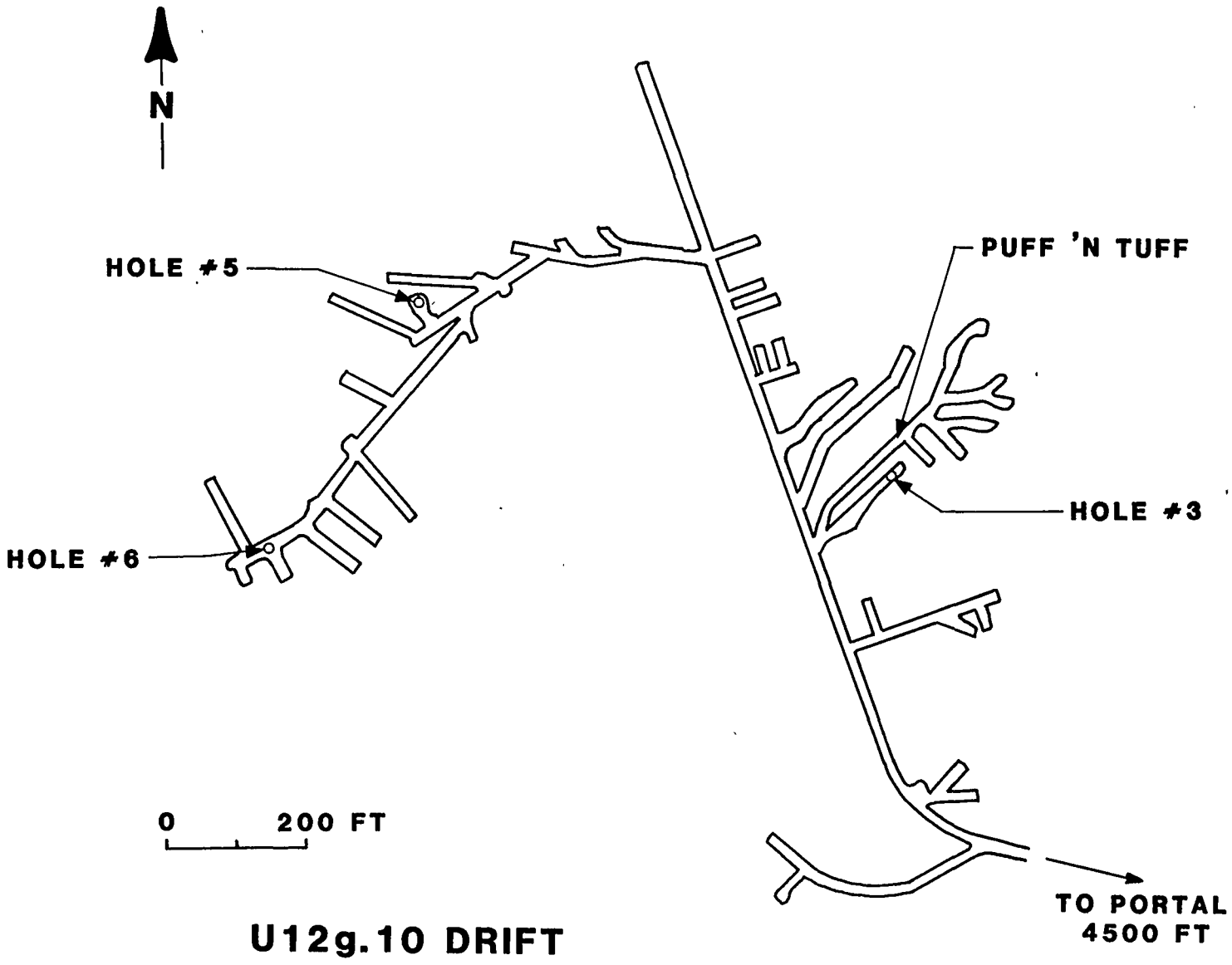

Figure 1. Ul2g.10 Drift Experiment Area

wedge-shaped fracture of constant height. Initially, it was hypothesized that the thickness of the boundary shale strata controlled fracture growth.[7] It was recognized, however, that the mechanical properties of the different reservoir rocks and the in situ stresses would influence the shape of the hydraulic fracture.[7-9] These effects cannot be quantitatively used for fracture design due to our present lack of understanding.

Studies to date have investigated the properties and conditions of the different strata and the interface between them. Daneshy[10] investigated the strength of the interface in laboratory fracturing experiments and found that a fracture would propagate across a well-bonded interface between dissimilar rocks. However, a weak interface, or an unbonded one, would arrest crack growth; an excellent example is the fracture termination at a "clean" coal seam/shale interface observed during fracturing to promote methane drainage of the seam prior to mining.[11]

Teufel[12] and Hanson et al.[13,14] performed laboratory experiments to study crack growth near both bonded and unbonded interfaces. They showed that, for unbonded interfaces, the stress normal to the interface (thus the friction along the interface and the ability to transmit shear) was the determining parameter for crack arrest or continued propagation. In experiments with bonded interfaces, Hanson et al.[13,14] determined that the strength of the two materials relative to the strength of the interface is important for crack propagation.

Simonson et al.[15] studied the effect that in situ stress variations have on fracture propagation. They showed that a layer of greater in situ stress would provide an effective barrier because of the increase in the fracturing pressure necessary to continue propagating a fracture in this layer. The effectiveness of the barrier would, of course, depend on the difference in stress in the two regions. They also showed that the upward or downward migration of the fractures can be influenced

by the hydrostatic gradient of the frac fluid relative to the vertical gradient of the minimum horizontal in situ stress. Cleary[16] suggested that an effective stress differential between the porous reservoir rock and the impermeable barrier can be obtained by drawing down the reservoir. This results in a reduced pore pressure and a reduced lateral confining stress so that the fracture would preferentially propagate in the lower stress reservoir rock.

Brechtel et al.[17] found significant differences in in situ stress between the Benson sandstone and adjacent shale layers, and they suggested treatment parameters to utilize this difference to control fracture height. Jones et al.[18] found considerable stress differences between various Devonian shale layers which might act as significant barriers. Hanson et al.[19] calculated an idealized stress field around lenses of different material properties from the surrounding formation and found that sizeable differences in in situ stresses should be expected under these conditions.

The problem of a fracture propagating in a brittle material such as rock has been analyzed using the concepts of linear elastic fracture mechanics. The success of this approach lies in the fact that for a single isotropic material the entire stress field near a crack tip can be described by a single parameter, K, known as the stress intensity factor. Since the mechanisms that govern fracture propagation behavior occur near the crack tip, it is easy to understand why K is the parameter that governs crack growth. The fracture criterion is simply that crack growth will occur when K reaches a critical value, K_{Ic}. Since K depends on the loading and crack geometry, this criterion says that a certain combination of load and crack size is required to cause crack growth.

The simplicity of a single parameter description of the crack tip stress field is lost when one considers a crack whose tip rests at a material interface. If the elastic moduli of the materials on either side of the interface differ, then the description of the stress field

requires two parameters. This situation is likely to require a more complex fracture criterion.

Many stress analyses have been performed on the problem of a crack approaching, reaching and passing through a material interface.[20-24] The stress analysis, however, is only part of the answer since without a fracture criterion one cannot predict when the crack will grow. The most obvious approach is to ignore the case of a crack whose tip rests at the interface and to examine the value of K as the crack tip approaches the interface and assume that crack growth simply requires a value of K equal to K_{Ic}.[15,20,25] This simplified approach leads directly to the prediction that a crack will be arrested in one material and will not even reach the interface if the second material has a higher modulus than the first. This results from the fact that for even a slight modulus increase the stress intensity factor goes to zero as the crack tip approaches the interface. In the opposite case, the fracture will cross the interface from a high modulus to a low modulus material, but immediately upon crossing it the stress intensity factor again goes to zero and fracture growth is terminated. Thus, in either case, fractures will not cross a material property interface. Obviously, the problem has been oversimplified since much experimental evidence, particularly for composite materials, refute these predictions.

One principal difficulty with these analyses is that the fracture criterion relies solely on the value of the stress intensity factor. K is defined as the strength of the square-root singularity in stress at the crack tip, but the nature of this singularity changes as an interface is approached. When the crack reaches the interface, the singularity is no longer square-root and K goes to zero; but the stresses remain singular (infinite). Other singularities now dominate the fracture growth.

In addition, the existing analyses do not include a model for the crack tip process zone. A model that describes the microcrack zone at

a crack tip is available[26] and could be used along with the stress analysis and a realistic fracture criterion. This might provide a more realistic assessment of the actual effect that material interfaces have on fracture growth.

While all of these theoretical studies and laboratory experiments offer insight to the problem of containment, it is clear that such idealized results are not easily applied directly. Direct evidence of fracture behavior under in situ conditions is necessary if the effects of the various possible controlling parameters are ever to be sorted out. Such information is necessary for both input into the modeling and analysis process and as a test of their predictive ability. Thus the intent of this study was to examine hydraulic fracture behavior near a material property interface where the results could be directly observed by mining. The observed results, correlated with the geological properties and physical parameters of the test would provide the necessary data to aid the modeling and analysis. Although the various volcanic tuffs in which these fractures are propagated are not the sandstones and shales usually encountered in gas reservoirs, proper application of rock mechanics principles allows the extrapolation of these results to gas well conditions.

DESIGN, DRILLING AND FRACTURING

The basic design of the experiment was to initiate fractures above and below a welded ash-flow tuff/ash-fall tuff interface and observe the behavior of the fractures at the interface by mineback. Using conventional fracture design calculations (i.e., ref. 27), a treatment was formulated with a sufficient volume of fluid so that fractures with an assumed height of 50 ft would have 300 ft wings. This is enough fluid volume so that the fractures would propagate to and "interact" with the interface. The frac fluid was a low water-loss class "A" cement so that the fractures would retain a large fraction of their

propagation width after pumping stopped and the cement set up. To allow for easy identification during mineback, different colored cements were used in each fracture. Calculated widths at the wellbore were 0.4 in in the ash-fall tuff and 0.15 in in the welded tuff.

Hole #6, with a collar elevation of 7555 ft was drilled to a total depth (TD) of 1455 ft. The entire hole was cored and a suite of logs was run. An ash flow unit, designated the Grouse Canyon Member of the Belted Range Tuff, was encountered from 1300 to 1352 ft. This member is comprised of an upper transition zone from 1300 to 1310 ft, a densely welded zone from 1310 to 1336 ft, and a lower transition zone from 1336 to 1346 ft. Below the ash flow unit is a peralkaline ash-fall tuff designated Tunnel Bed 5. This experiment utilizes the contact between Tunnel Bed 5 and the dense welded zone of the Grouse Canyon Member for the interface; however, the interface is not discrete since the variation in properties occurs over a transition zone which is several feet wide. All interfaces are well bonded. A general stratigraphic description of the experiment region is shown in Table 1. The lower transition zone is shown in particular detail because the principal property differences which were exploited for this experiment occur there. In general, the densely welded and vitric zones of the ash-flow are hard, high modulus rocks whereas the ash-fall tuffs and the matrix of the rubble flow zone are soft, low modulus materials. The basal zone of the ash-flow is intermediate and variable. Other information on geology, material properties and in situ stresses is given in Reference 5.

The physical properties of eight core samples from this region of Hole #6 are shown in Table 2. The density, tensile strength, elastic moduli and acoustic velocities of the welded tuff are much larger than the respective properties of the ash fall tuff and the porosity is considerably less. Physical properties were also calculated from the 3-dimensional velocity log. These results are plotted in Figures 2 and 3

TABLE 1

Brief Stratigraphic Description of The Interface Section

Near Hole #6

Tuff Type	Zone		Thickness	Brief Description
Ash Fall			200	White to brown ash fall tuff and reworked ash fall tuff
Ash Flow	Upper Transition		10-12	Orange to brown, partially welded ash flow tuff; occasionally fractured
	Densely Welded		30-35	Red, brown, and gray densely welded, devitrified ash flow tuff; highly fractured
	Lower Transition Zone	Rubble Flow	0.5-3	Assorted sub-angular to sub-rounded igneous lithic fragments (<1 mm to 45 cm) in a crypto-crystalline, poorly indurated, orange and gray matrix
		Vitric	2-4	Greenish-brown, black and brown welded ash flow tuff, mostly vitric; moderately fractured
		Basal	1.5-2.5	Gray to brown, partially welded ash flow tuff and an intermittent brown lithic-rich flow; occasionally fractured
Ash Fall			100	Greenish yellow, peralkaline ash fall tuff; zeolitized; massive
Ash Fall			1000	Other ash fall tuffs of varying properties

TABLE 2

PHYSICAL PROPERTIES FROM CORE SAMPLES OF HOLE #6

DEPTH (ft)	TYPE	BULK DENSITY (gm/cc)	GRAIN DENSITY (gm/cc)	POROSITY (%)	TENSILE STRENGTH (psi)	MODULUS OF ELASTICITY (million psi)	POISSON'S RATIO	P WAVE VELOCITY (ft/sec)	S WAVE VELOCITY (ft/sec)
1297	Ashfall	1.95	2.49	35.0	35	1.22	0.213	9450	4870
1305	Transition	2.12	2.62	28.7	126	2.12	0.218	10100	5510
1313	Transition	1.92	2.63	40.3	108	0.80	-	7900	4430
1323	Densely Welded	2.42	2.65	12.8	820	5.07	0.213	14670	7080
1339	Transition	2.18	2.63	25.7	555	2.35	0.194	10800	5880
1343	Transition	2.14	2.47	20.1	29	2.20	0.265	11540	6280
1354	Ashfall	1.67	2.42	49.2	20	0.81	0.322	6190	3450
1363	Ashfall	1.68	2.42	48.6	39	0.30	0.206	5160	3130

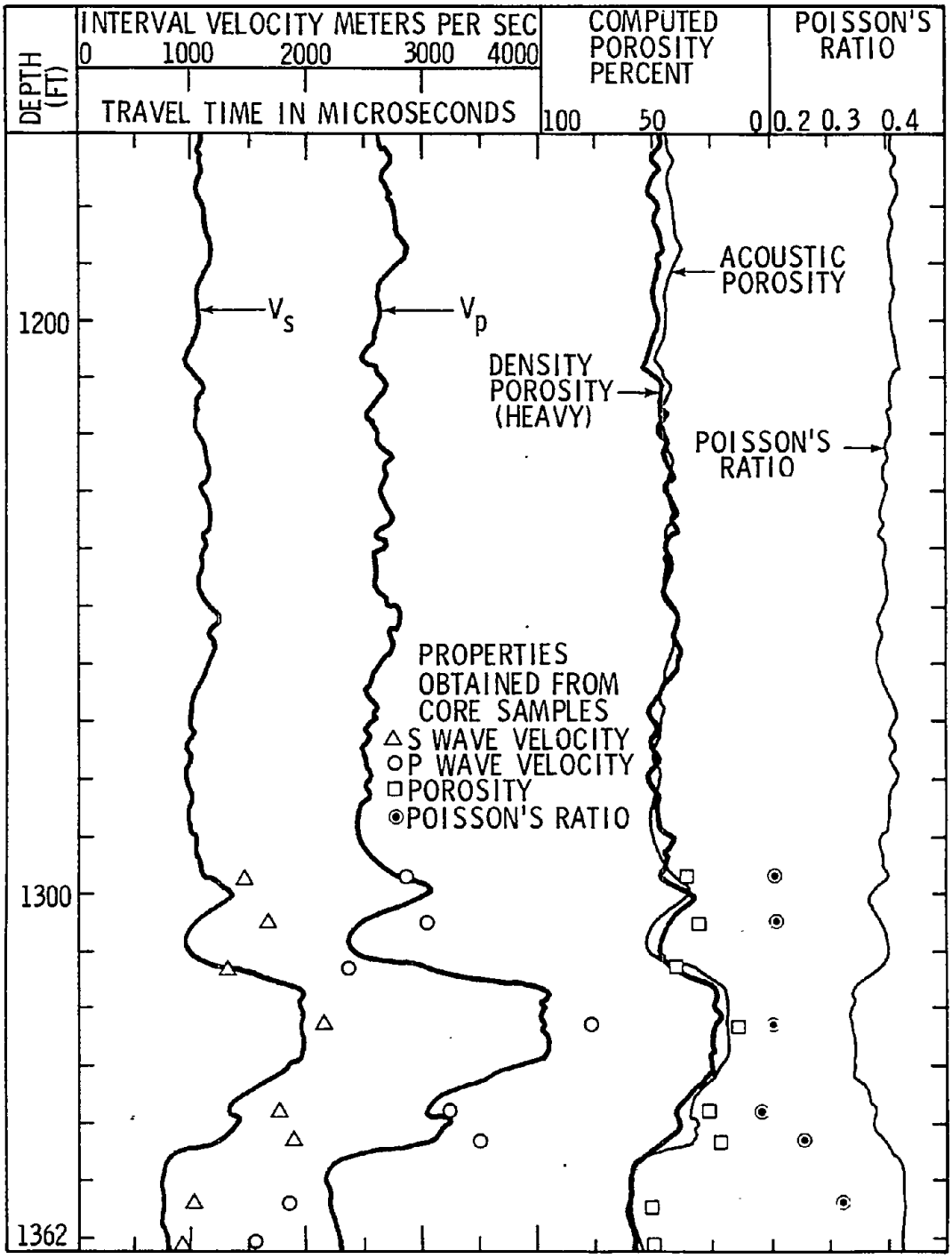

Figure 2. Log-Calculated Properties and Properties Measured From Core

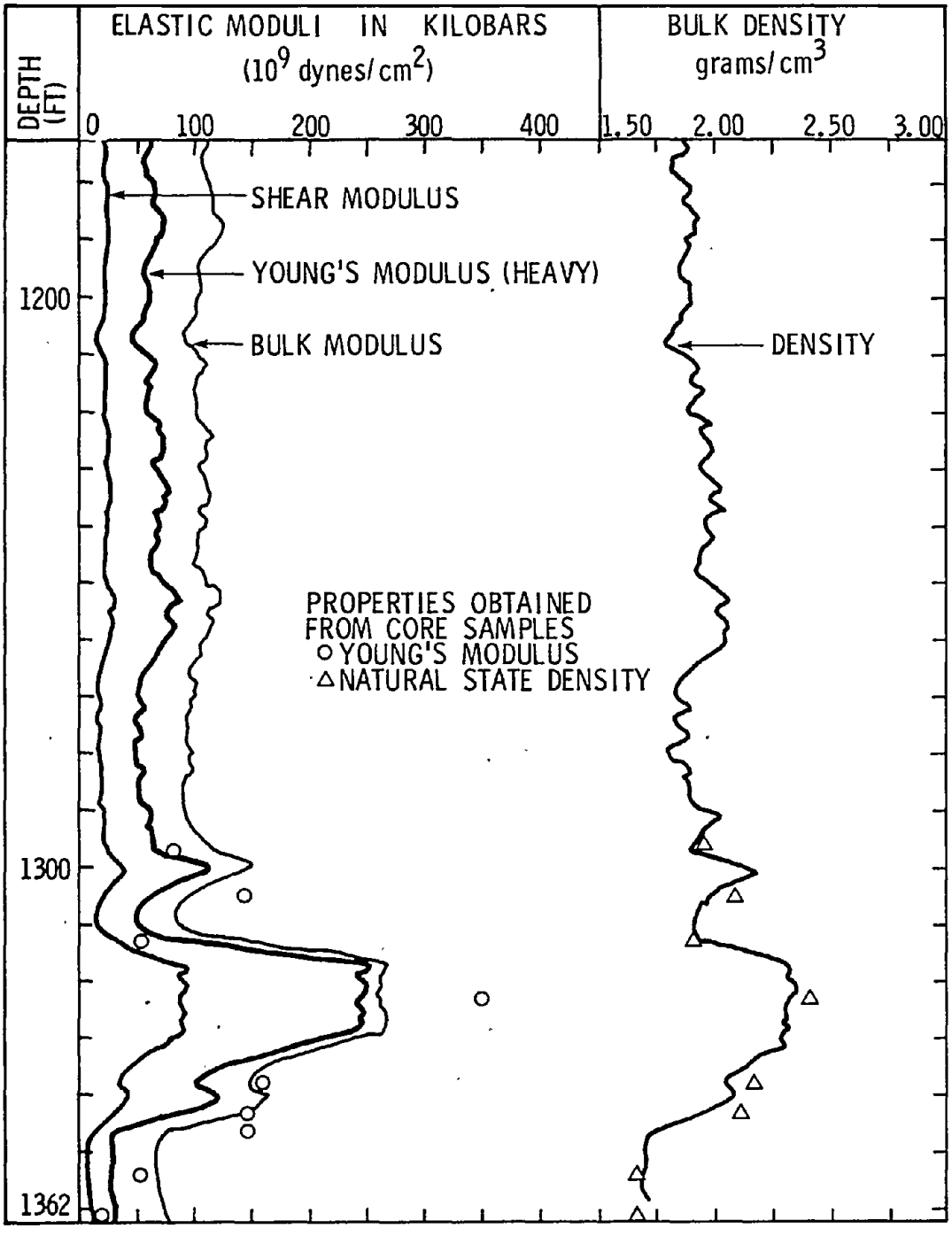

Figure 3. Log-Calculated Properties and Properties Measured From Core

and are compared with the laboratory results. Only Poisson's ratio shows a poor correlation.

The treatment in the ash fall tuff, which is below the interface, was performed in August 1977. As shown in Figure 4, pea gravel was spotted to 1358 ft and an inflatable packer was situated with the bottom of the element at 1352 ft. The 6 ft open zone was fractured through NQ tubing (2 3/8 in ID) at 6 bbl/min with 5000 gal of green grout followed by 4000 gal of black grout. The complete pumping schedule is shown in Table 3. Bottom hole pressure and flow rate were recorded, but a wellhead pressure transducer malfunctioned. The flow rate, bottom hole pressure and seismic data are shown in Figure 5. As seen in Figure 5, several shut-in periods during fracturing were required because of leaks and equipment malfunctions.

The welded tuff zone was treated in October because of delays due to lost pipe. At that time the hole had been reamed from 4 to 6 1/4 in and TD was tagged at 1368 ft. As shown in Figure 6, the hole was backfilled with pea gravel to 1331 ft and the packer was set at 1324.5 ft. The formation was broken down with 30 bbl of water, shut in for a quiet period for acoustic signal detection, and treated with 5000 gal of blue-gray grout at 6 bbl/min through HQ tubing (2 7/8 in ID). The flow rate, well head pressure and bottom hole pressure from an Amerada bomb and a Hewlett-Packard (HP) quartz crystal oscillator transducer were recorded for both breakdown and the treatment. The data from this fracture are shown in Figures 7 and 8.

Mineback Results

The mineback of the fractures was conducted intermittently between September, 1977 and July, 1978. The overall mineback area of the Hole #6 fractures is shown in Figure 9. The mining between points A and B was an access drift up to the level of the interface and occurred between September and November. Several coreholes were drilled from

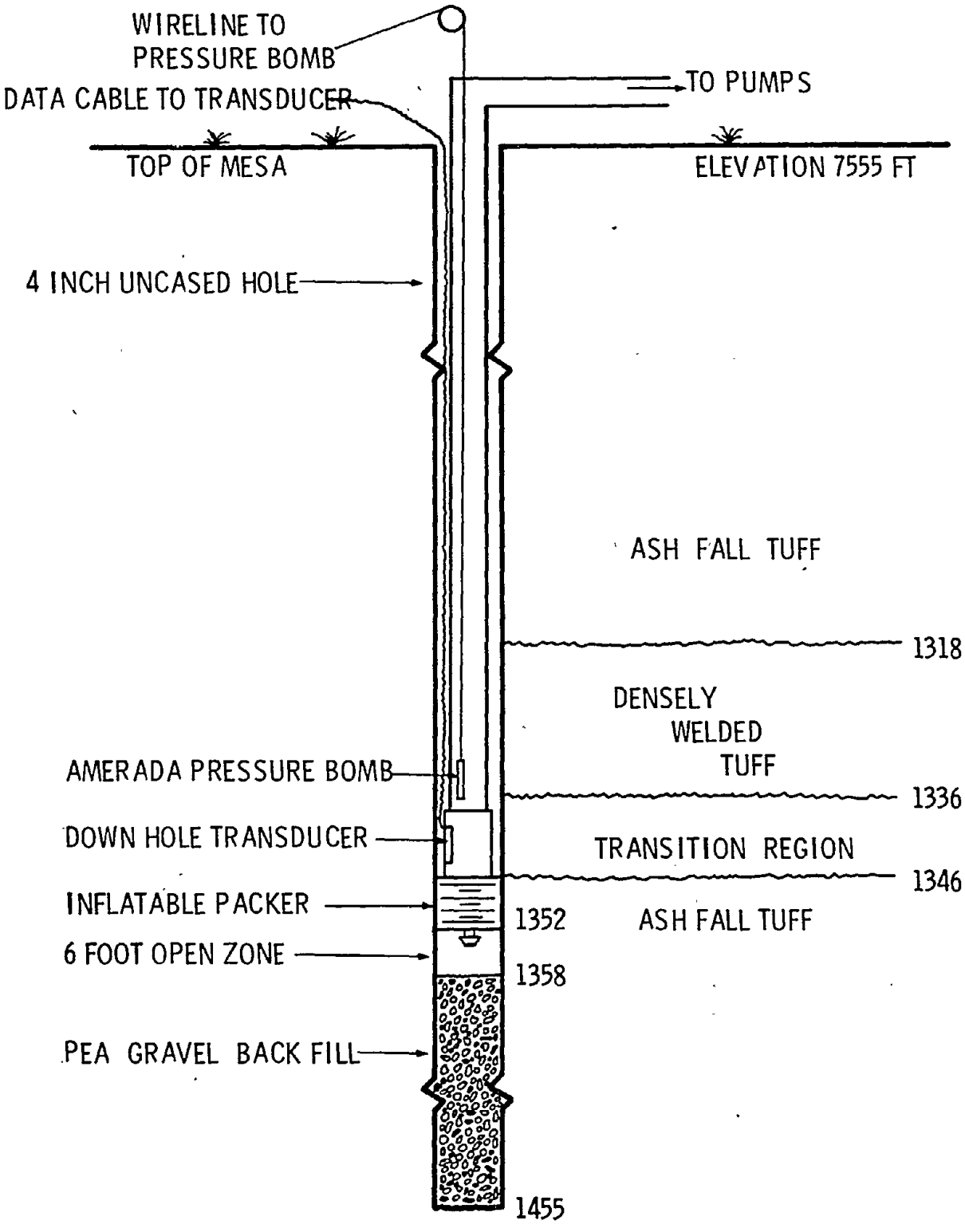

Figure 4. Ash Fall Tuff Hydraulic Fracture Zone

TABLE 3

Treatment Schedule

Fluid: Nevada "A" Cement @ 15.4 lb/gal

Viscosity: 128 cp ($n' = 0.86$, $K' = 0.0031$ lb-sec$^{n'}$/ft^2)

($\eta = 0.07$ lbm/ft-sec, $\tau_y = 0.23$ lb/ft^2

Flow rate: 6 bbls/min

ASH FALL TUFF

Breakdown	1260 gal Water
Stage 1	5000 gal Green Cement
Stage 2	4000 gal Black Cement
Displacement	420 gal Water

WELDED TUFF

Breakdown	1260 gal Water
Fracturing	5000 gal Blue Cement
Displacement	420 gal Water

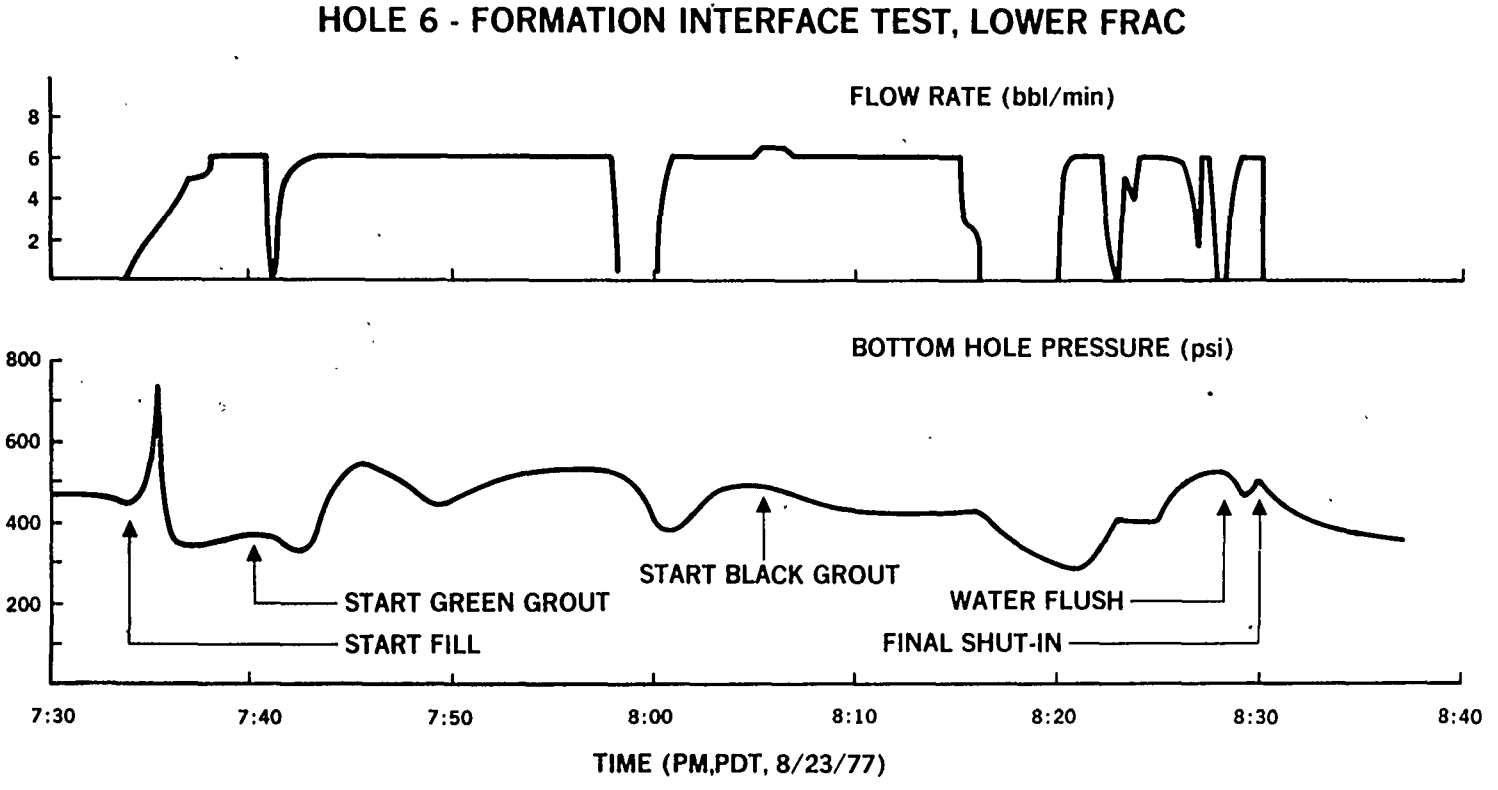

Figure 5. Pressure and Flow Rate During Fracturing in Ash-Fall Zone

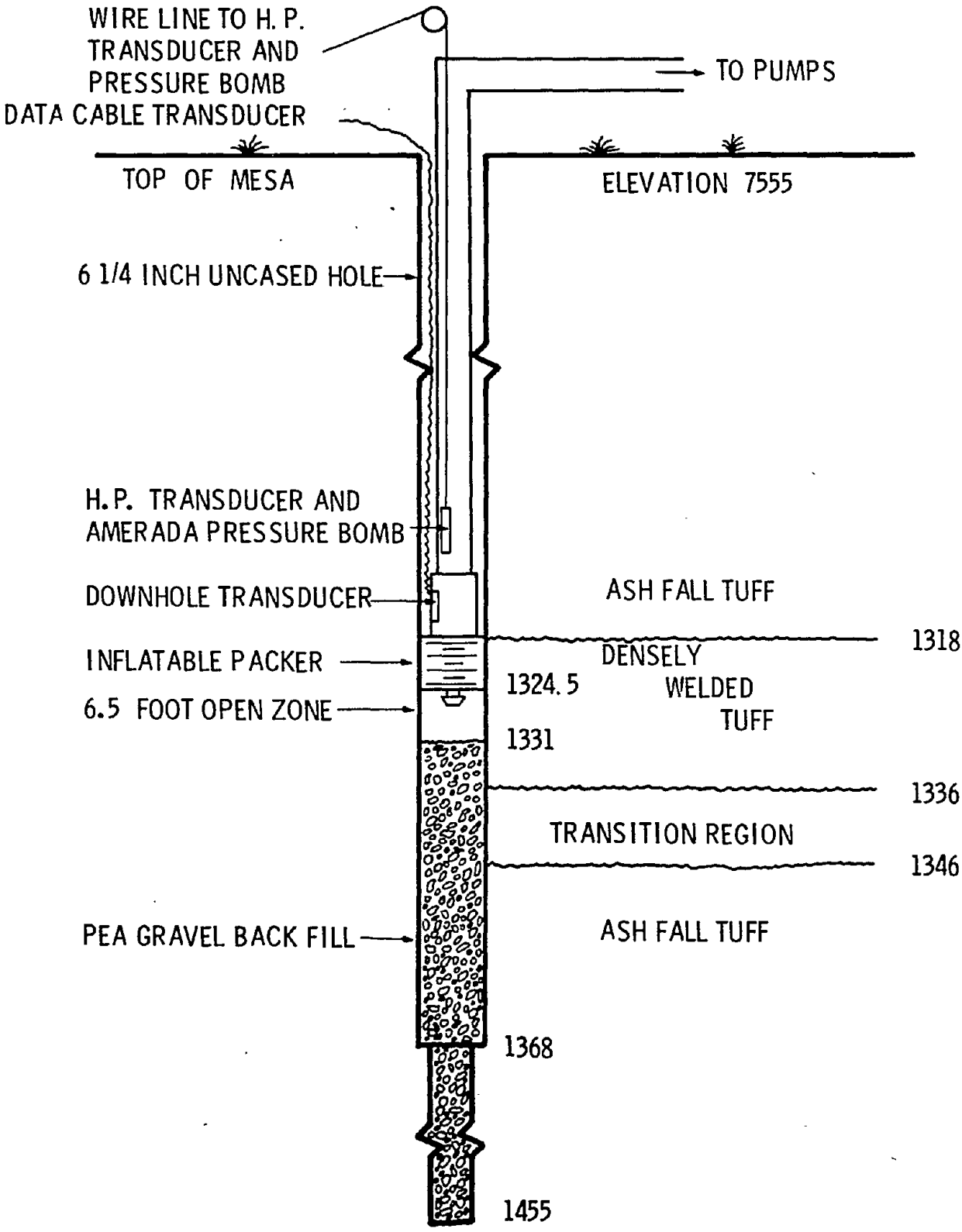

Figure 6. Welded Tuff Hydraulic Fracturing Zone

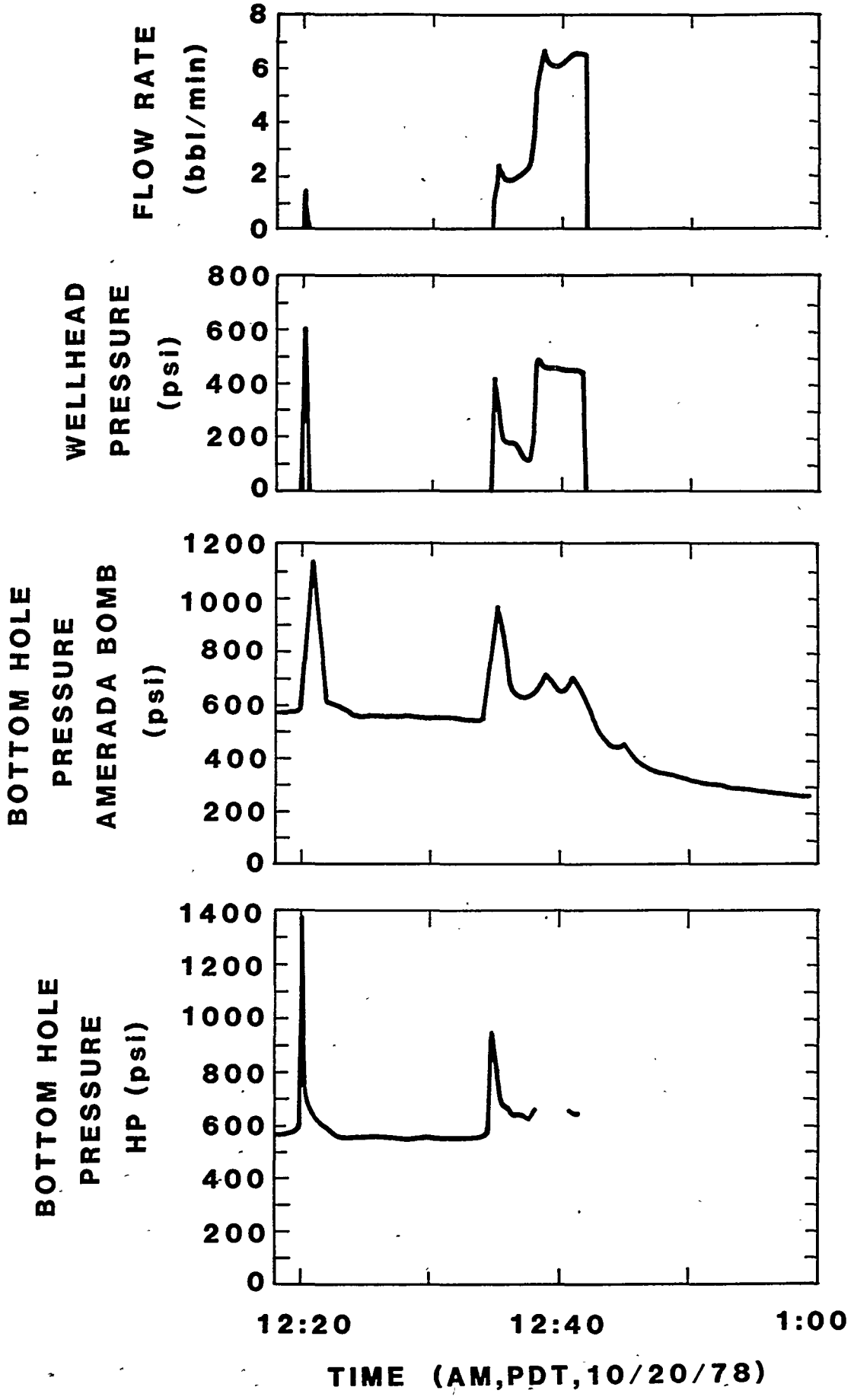

Figure 7. Pressure and Flow Rate During Breakdown in Welded Tuff Zone

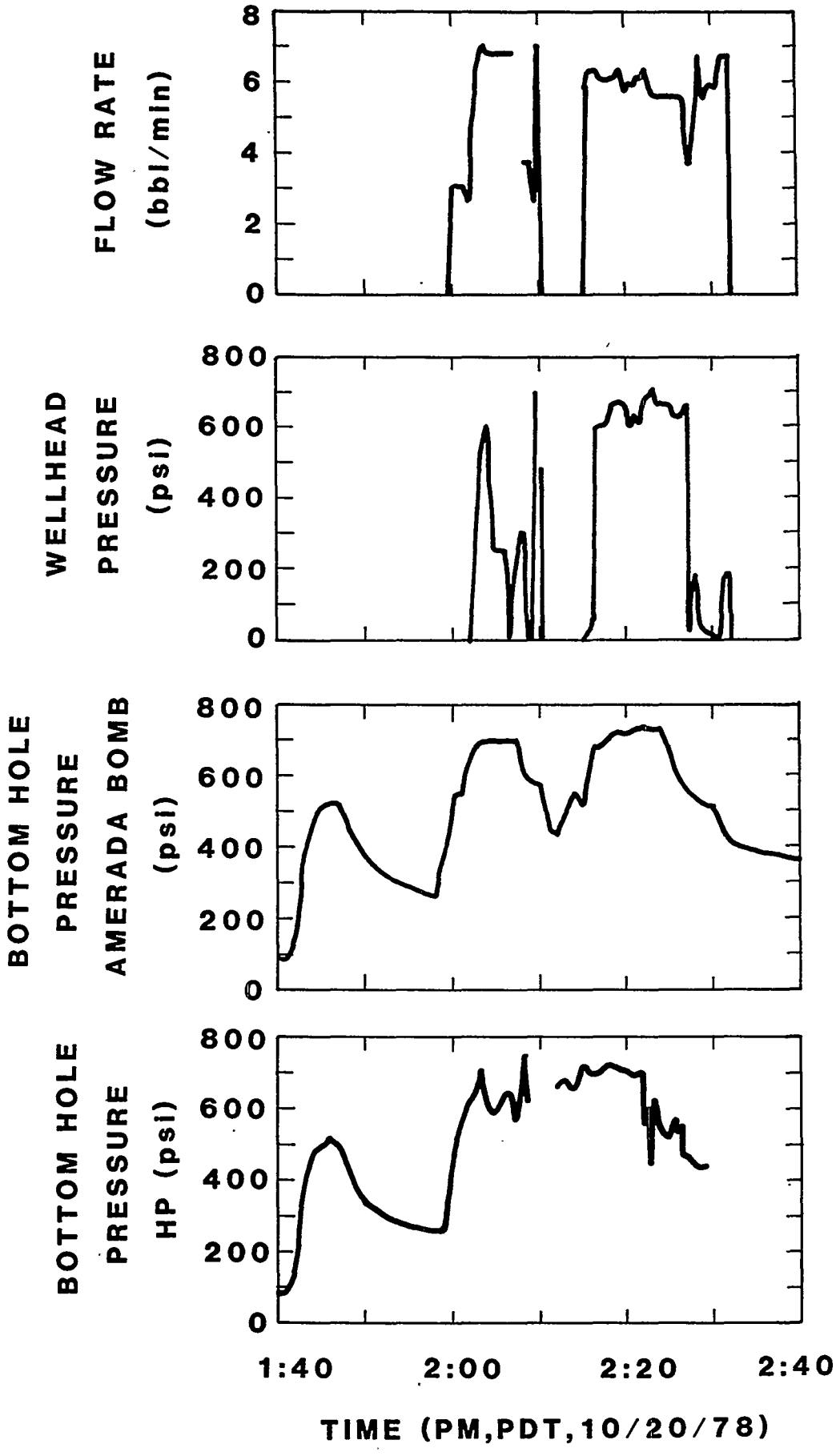

Figure 8. Pressure and Flow Rate During Fracturing in Welded Tuff Zone

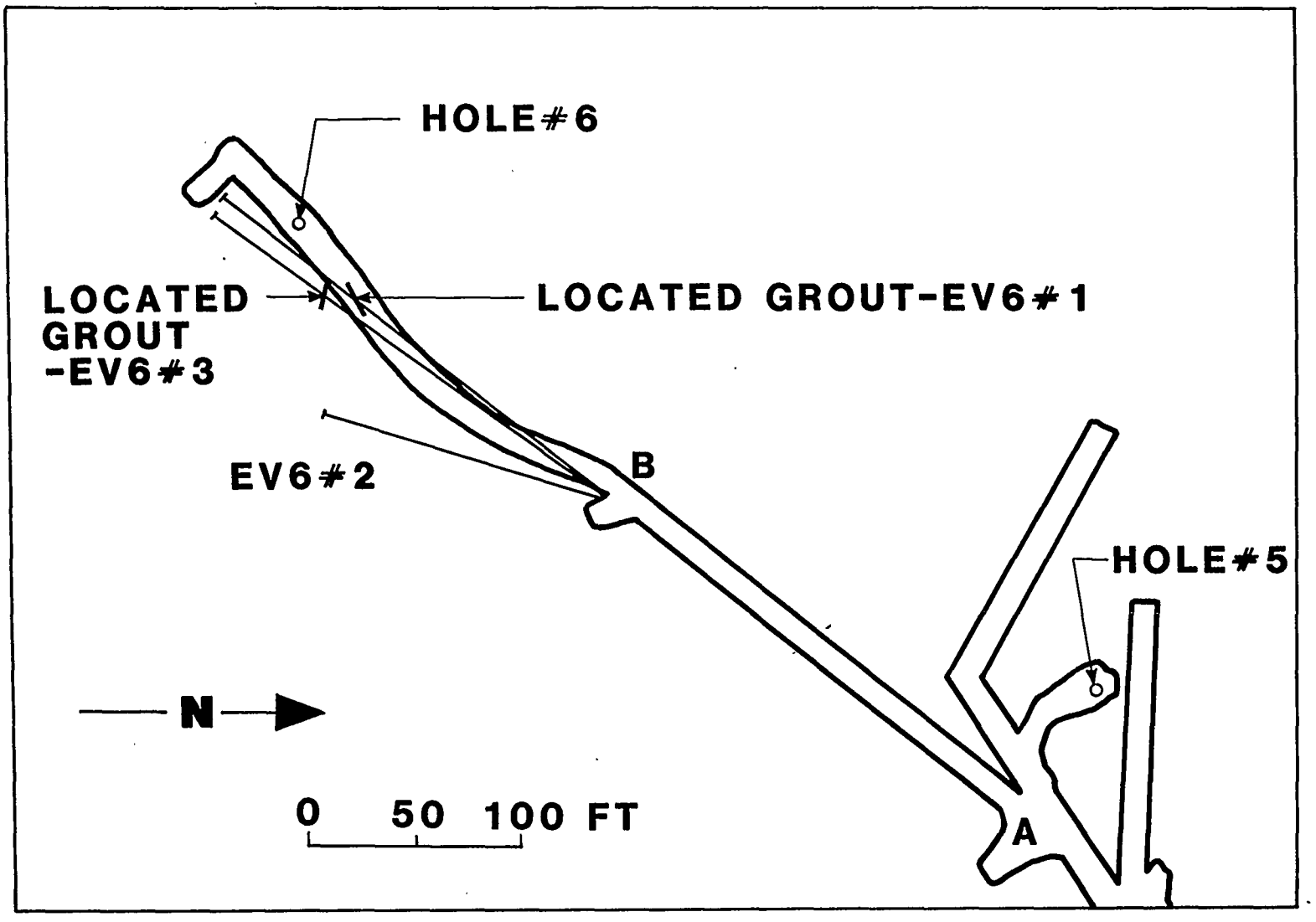

Figure 9. Plan View of Hole #6 Experiment Area

point B to locate the fractures and then mineback proceeded to uncover the entire extent of the fractures at the level of the interfaces. Geologists performed detailed mapping and photographing of the induced fractures and important geological features throughout this entire region.

The fracture was first observed at 425.4 ft into the mineback which corresponds to 91 ft to the NE of the borehole. This location is 2-4 ft past the tip of the fracture on this wing. As shown in the photograph and mining face map of Figure 10, the fracture has about a 60° NW dip at this point, trends N60°E, and has a width of < 1 mm at the top and ~3 mm at the bottom of the face. The cement is entirely green at this location. At the top left-hand corner of the figure, the fracture can be seen crossing the interface which is marked by a fairly continuous iron stained band. Throughout the mineback region, the interface strikes N45-60°E and dips 5-13° NW. The propagation of the fracture through the interface resulted in no apparent change in orientation or character other than a decrease in fracture width. Several en echelon fracture strands can be seen at the top and bottom. Parallel strands and en echelon features are common in nearly all fractures conducted in G-tunnel.

At the 436.5 ft location or 78 ft from the borehole, the green fracture is as shown in Figure 11. The width of the fracture is 1-2 mm near the back (roof), 3-4 mm in the center and 4-5 mm near the invert (floor) of the mineback. At this location the fracture dips about 65° NW and trends N65°E. Near the upper left of the photo the fracture can be seen crossing the interface. The apparent offset of the fracture (in the photograph) is due to an irregular rock slab which was disjointed, upsetting the surface continuity. In fact, the fracture is continuous.

Figure 12 shows the fracture at 449.9 ft or 66.5 ft from the borehole. The photograph shows a close up at the interface. At this point the fracture dips 62° W near the back and 72° W near the invert

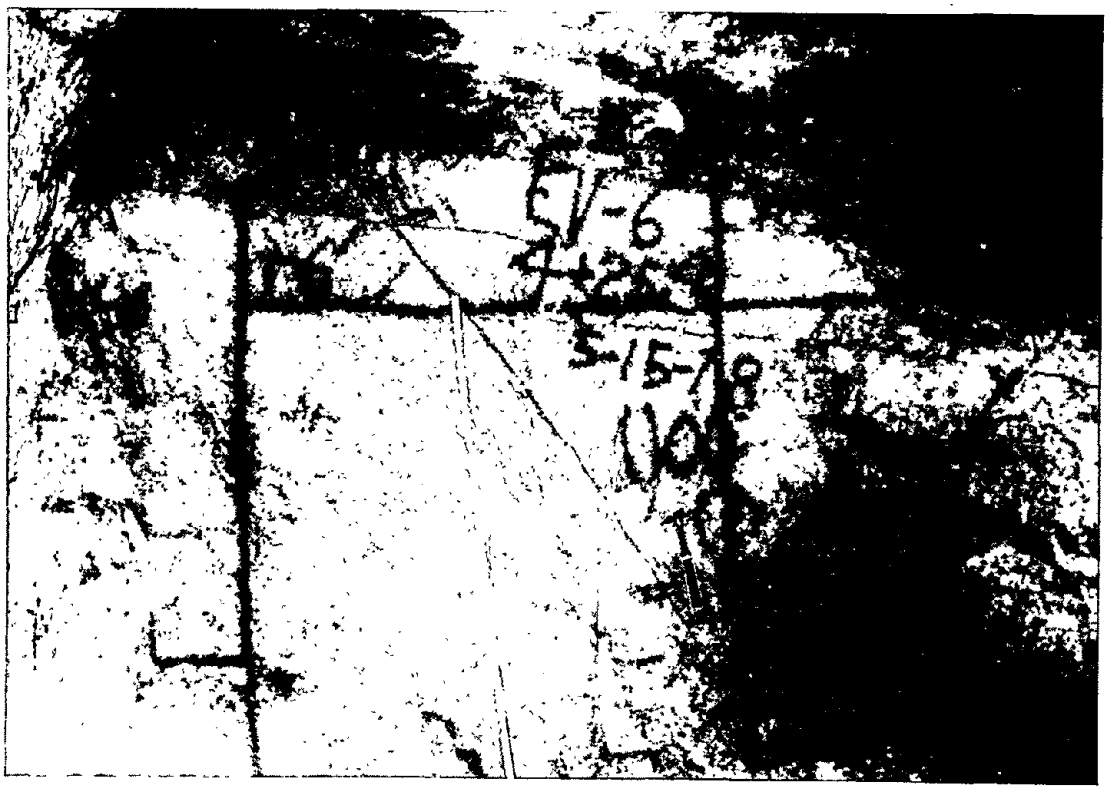

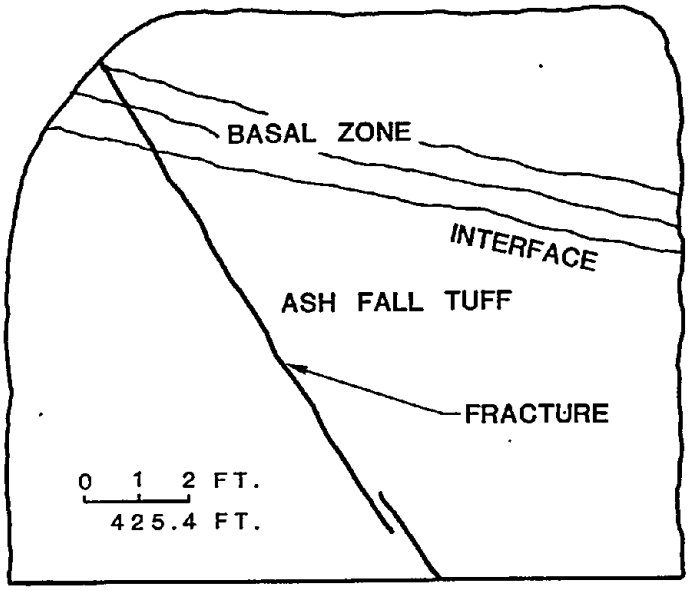

Figure 10. Photograph and Face Map at 425.4 ft in Mineback

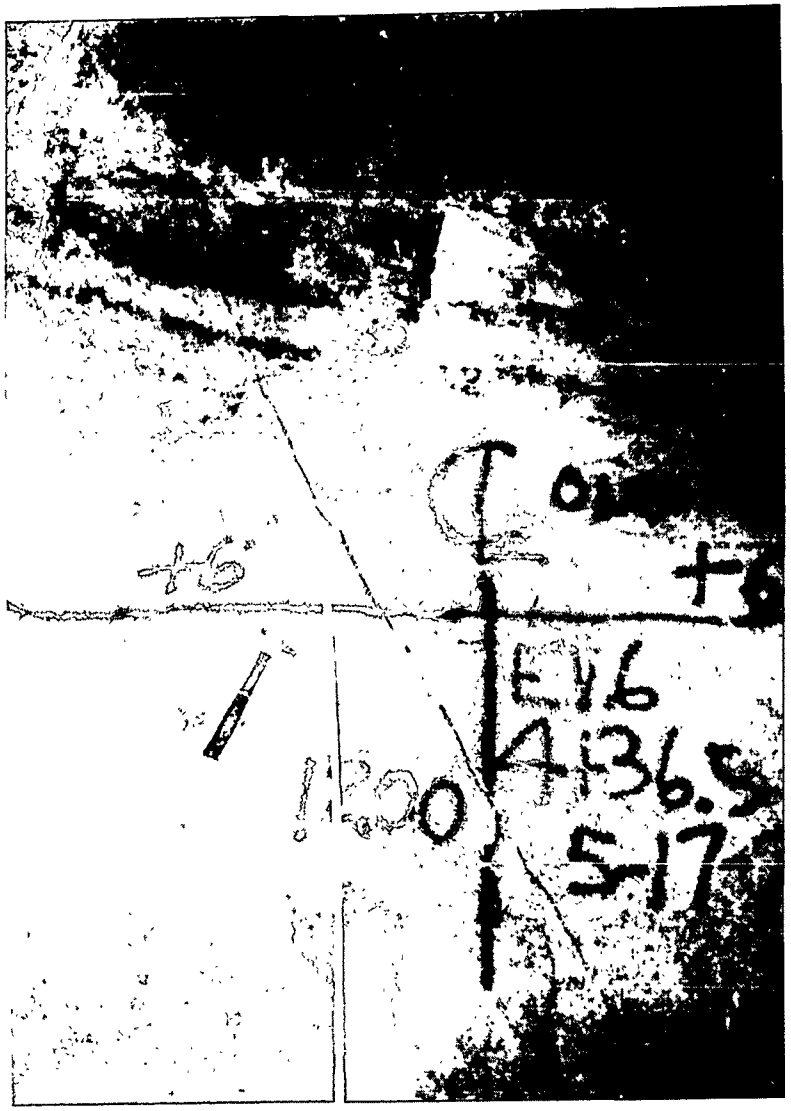

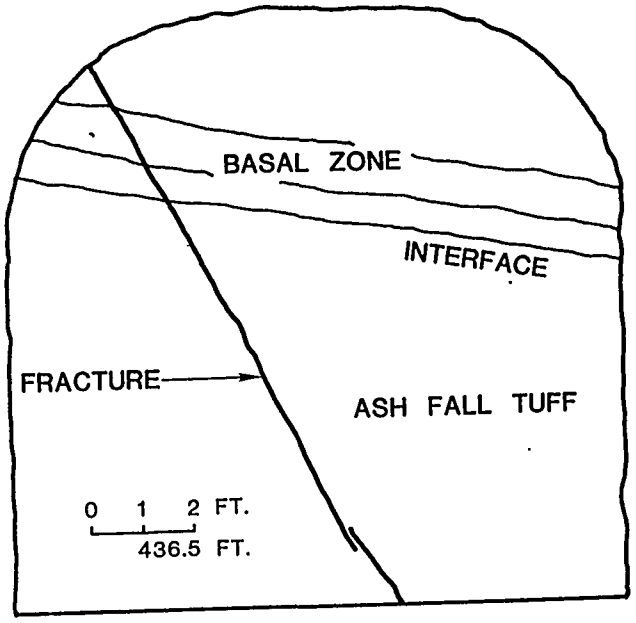

Figure 11. Photohraph and Face Map at 436.5 ft in Mineback

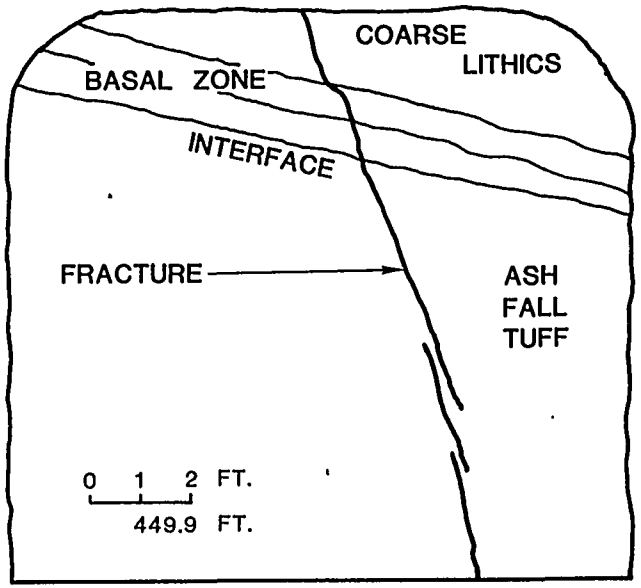

Figure 12. Photograph and Face Map at 449.9 ft in Mineback

and strikes N50°E. The width ranges from ~3 mm above to 5-6 mm below the interface. The fracture is predominantly green with some black, but both colors of grout appear as separate streaks. It appears as if the green grout had partially solidified before the black cement reached this point.

At the 461.2 ft location or 53 ft from the borehole the fracture has a strike of N55°E and a dip of 73°NW. It is becoming more vertical closer to the borehole. As shown in Figure 13 a relatively greater portion of the ash-flow tuff was exposed as the mining progressed. At this location the fracture changes character considerably at the lowest unit in the ash-flow tuff. However, it appears that the induced fracture joined a natural fracture in this layer. Several more of these small natural fractures appear to the right of the induced fracture. The hydraulic fracture is mostly green with about 20% black grout and some apparent mixing to dark, grayish green. The thickness varies from 3-6 mm above the interface to an average of 5 mm in the ash-fall tuff with variations of from 4-10 mm.

The fracture at 479.5 ft or 35 ft NE of the borehole is shown in Figure 14. The fracture stikes N55°E and dips 79°NW. Fracture width varies from 4-5 mm above the interface to 4-10 mm below with an average of 5 mm below. The fracture is about 60% black with some apparent mixing of green and black cement. The fracture readily crosses the interface but its course is disrupted at this location by a hard lithic about 18 in above the interface. The fracture apparently approached the lithic from below, intercepted it and veered around it continuing upward. This would seem to indicate that the fracture propagated upward through the interface at this location rather than through both layers simultaneously, outward from the wellbore.

At 494.4 ft or 20 ft from the wellbore, the fracture has divided into three strands as shown in Figure 15. This appears to be a fairly common, yet local, phenomenon and separate strands may exist for only

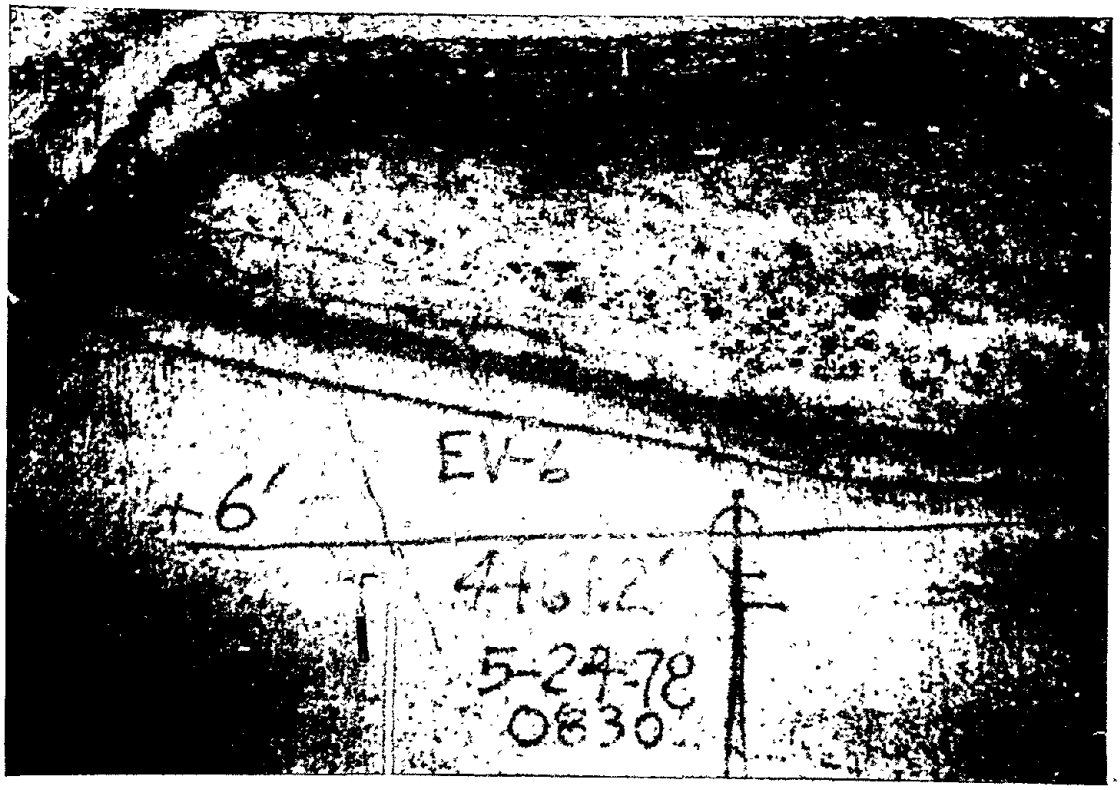

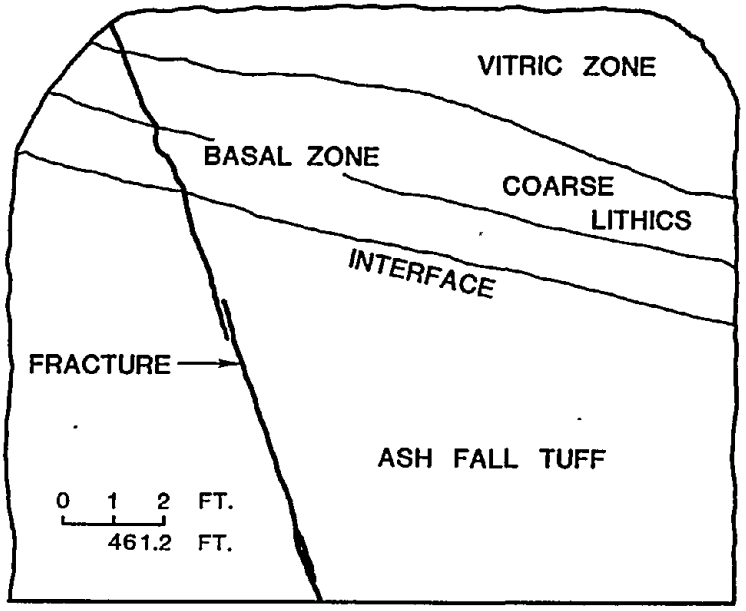

Figure 13. Photograph and Face Map at 461.2 ft in Mineback

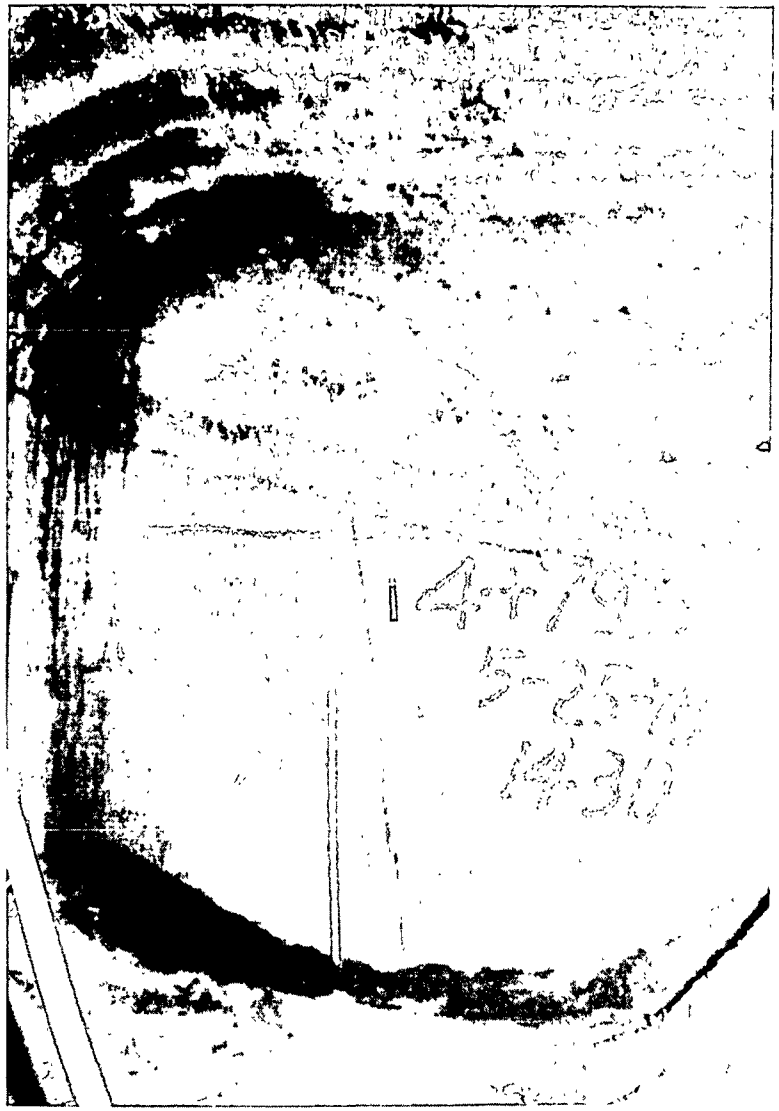

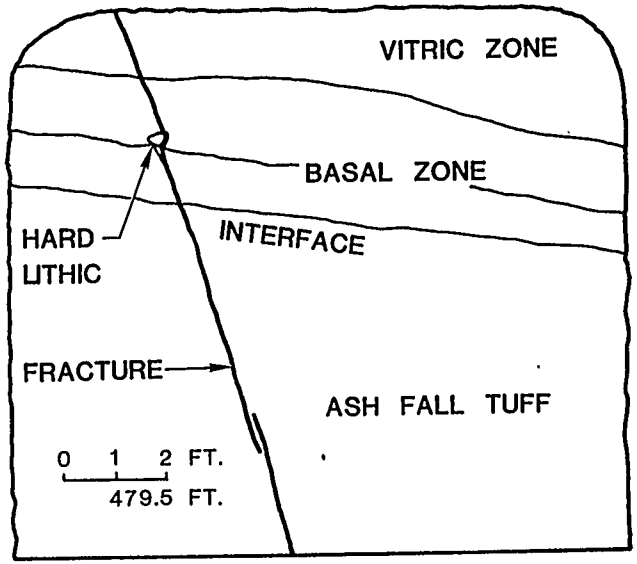

Figure 14. Photograph and Face Map at 479.5 ft in Mineback

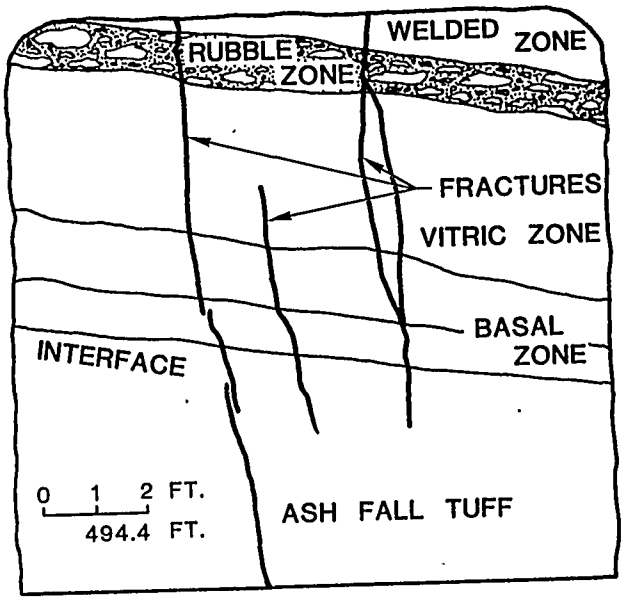

Figure 15. Photograph and Face Map at 494.4 ft in Mineback

a few inches or for several feet. The strand on the left appears to be the "main" fracture and it has a dip of 85°NW and trends N55°E. The fracture is mostly green near the back and mostly black in the ash-fall tuff with some green and gray. The gray cement is from the fracture initiated in the welded tuff about two months after the green and black fracture treatment was conducted. (Apparently this grout is gray because there was insufficient blue dye added. Occasionally the gray cement has a blue tint). The main fracture width averages 5-6 mm above the interface and 10 mm below. The other strands are each 2-3 mm wide with mostly gray grout. At this location, fracture behavior in the rubble flow zone is inconsistent. As shown in Figure 16, the fracture may either intersect a lithic or meander around them. The interaction with the lithics appears to be random.

Figure 17 shows the fracture at 512.9 ft or 1.5 ft from the borehole. Here the entire transition zone is exposed; the ash-fall tuff is at the very bottom and the densely welded tuff is at the top of the photo. The fracture readily breaks through the entire transition zone and into the welded tuff which has at least a factor of ten increase in modulus over the ash-fall tuff. The fracture dips 88°SE with a trend of about N45°E. The fracture is filled with about 70% black cement, mostly in the center with ~10% green near the walls and the rest gray. The width varies from 1-10 mm with an average of about 7 mm. There appears to be a natural fracture in the vitric layer which the fracture intercepted and propagated through.

The borehole is shown in Figure 18. This is a photograph looking up at the borehole in the welded tuff. It should be remembered that after the first fracture was conducted, the hole was reamed from 4 in to 6.25 in in order to recover some lost tools. Afterward the hole was backfilled with pea gravel to a point about 10-15 ft above this photo. When the second fracture was conducted, the grey grout seeped through the gravel and what is seen now is gravel and cement fill from

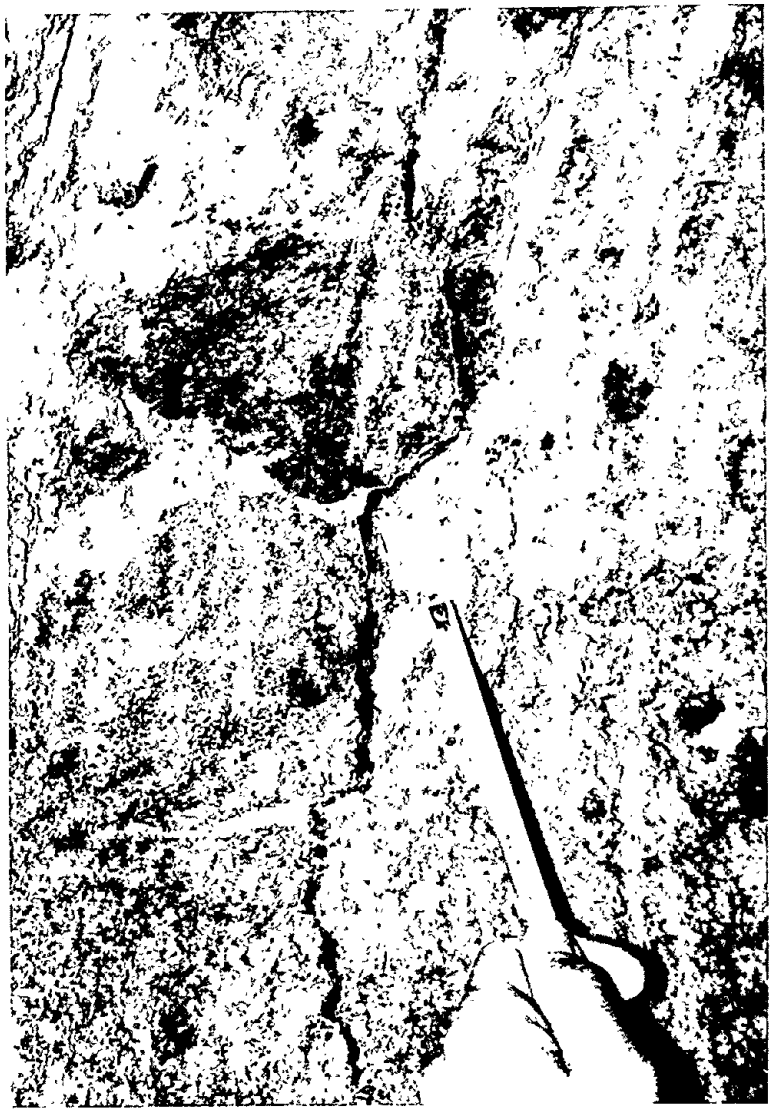

Figure 16. Photograph of Fracture Behavior Near Hard Lithics

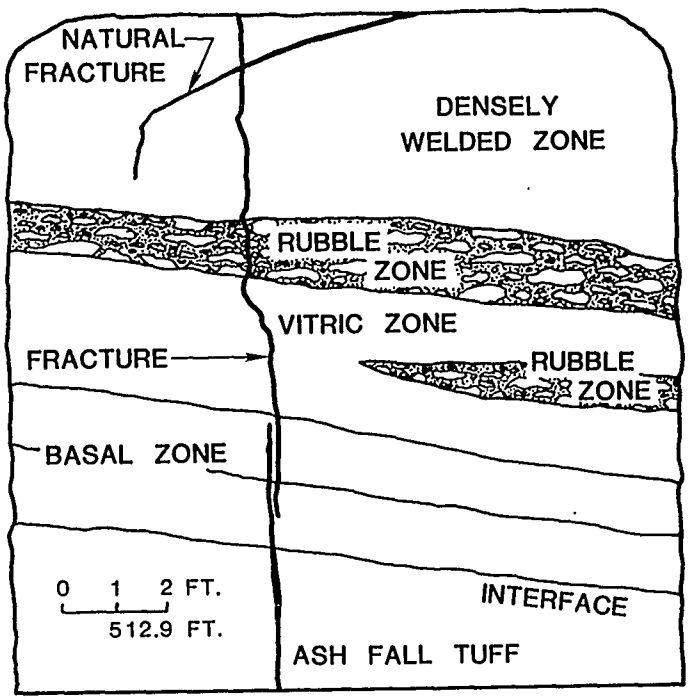

Figure 17. Photograph and Face Map at 512.9 ft in Mineback

Figure 18. Photograph of Fracture Initiating from Borehole in Welded Tuff

the second fracture. Although the green and black fracture apparently intersects the hole here, it would have only barely intersected the original 4 in hole, if at all. Since this is above the packers, one would have expected some indication in the annulus during the treatment if grout was by passing the packer, but none was seen. The day after this treatment there was also no trouble lowering tools to the depth of the welded tuff so very little grout filled the hole. It is very possible that the fracture did not intersect the wellbore at this elevation. At this location (about 20 ft above the open hole zone where this frac initiated) the width is 2-7 mm, averaging about 5 mm. It is mostly black with some green and very little, if any, gray.

Nearly every location where the fracture crosses a natural fracture the induced fracture is offset. Offsets greater than one foot have been observed in the welded tuff. In general, the welded tuff is uniformly highly fractured although some less fractured areas have been observed. The overall transition zone is occasionally fractured, but in several locations the hard vitric unit is highly fractured. The ash-fall tuff is very competent.

Figure 19 shows the fracture at 516.1 ft or 1.5 ft past (SW of) the borehole. The borehole can be seen near the back where it appears as an ellipse because of the curved mineback surface. The fracture here is approximately vertical and trends N53°E. The grout is mostly green and black. The dark vitric unit near the lower center of the photograph is highly fractured at this location as is obvious in the photo. Fracture widths varies from 1-2 mm in the ash fall tuff at the very bottom, 3-5 mm in the vitric unit and, surprisingly, 8-10 mm in the welded tuff. It is not clear why the width in the welded tuff is so large at this location. The open-hole zone where the first fracture was initiated is 15-20 ft below the invert at this location.

At 523.8 ft or about 9 ft SW of the borehole the fracture consists of several strands as seen in Figure 20. The prominent fracture on the

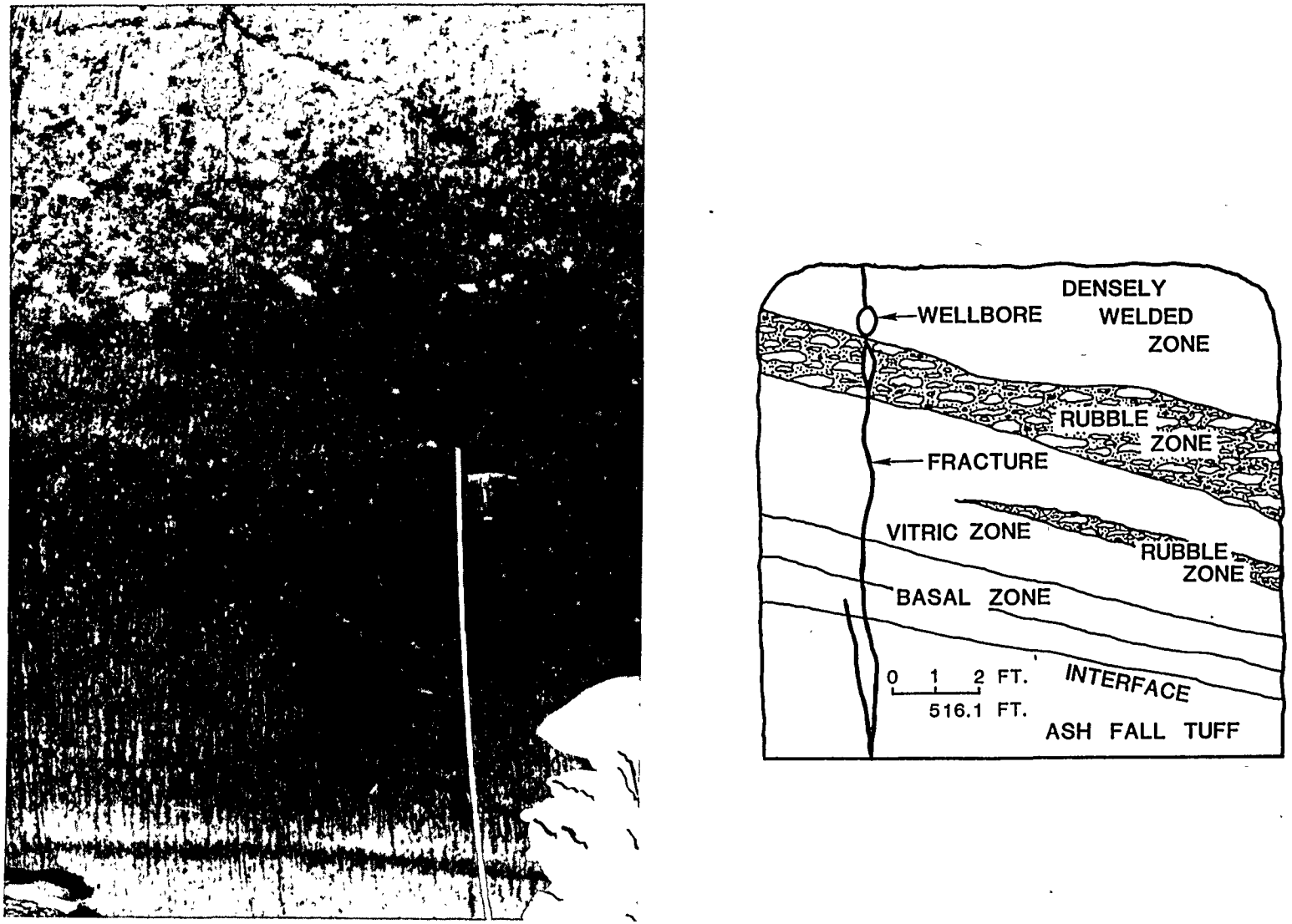

Figure 19. Photograph and Face Map at 519.1 ft in Mineback

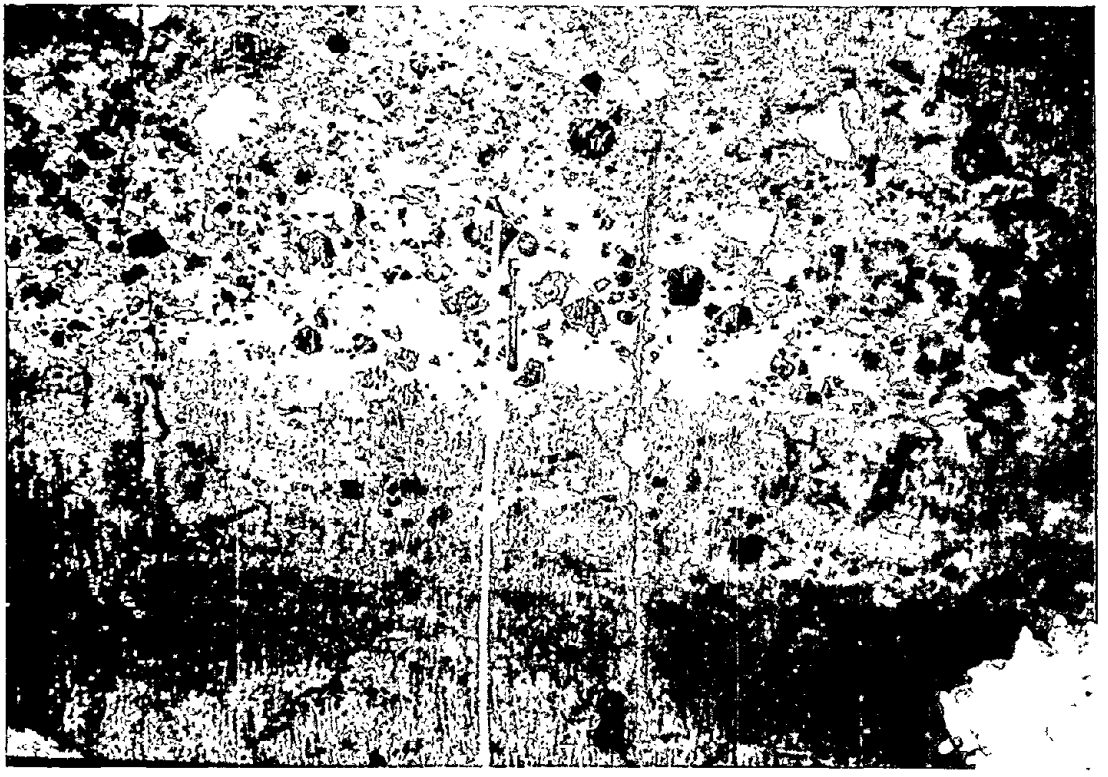

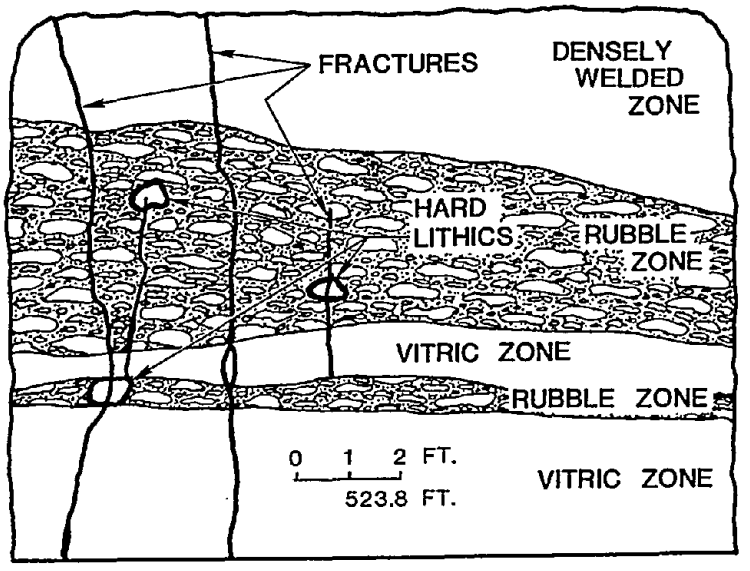

Figure 20. Photograph and Face Map at 523.8 ft in Mineback

left has a dip of 68°SE near the bottom and 82°NW near the top with a strike varying from N50°-60°E. The thickness varies from 1-2 mm in the lower hard vitric zone to 5-7 mm in the soft rubble zone. This fracture is mostly green and black with black on the inside. The small fracture just slightly to the right is mostly green and it terminates in the large, light-colored lithic at the top left. The fracture in the left center is mostly gray grout with some green on the outside, having a width of 1-3 mm. A hairline fracture in the center splits a dark hard, lithic in half.

The fracture at 535.9 ft or 21.5 ft past the borehole is shown in Figure 21. The photograph shows only the top, left-hand corner of the mineback face. Of particular interest is the behavior of the fracture in the highly fractured welded tuff. The fracture is often offset several inches by the natural fractures which cross its path. Here the upper fracture strand is 3-5 mm thick and is filled with green grout. The lower frac strand is 5-10 mm wide and is mostly black grout with a trace of green. The fracture dips 77-84°NW.

Figure 22 shows the fracture at the 549.5 ft location or 35 ft past the borehole. At this point the entire transition region can again be seen with the ash-fall tuff at the bottom and the welded tuff just above the rubble zone. The fracture has an orientation of N60°E, 90° and contains green and black grout which is 3-8 mm wide. Some gray grout is seen in the hairline secondary fractures. This is one of the few locations where natural fractures in the transition zone were seen penetrating into the ash fall tuff. The fracture intersected one of these natural fractures creating an apparent slight offset just above the interface at the bottom of the photo.

At 567 ft or 52.5 ft past the borehole and 7 ft from the tip, the fracture narrowed to a width of 2-3 mm filled with green and gray grout. As shown in Figure 23, the exposed fracture also extends from the ash-fall tuff, through the interface and into the welded tuff. In two

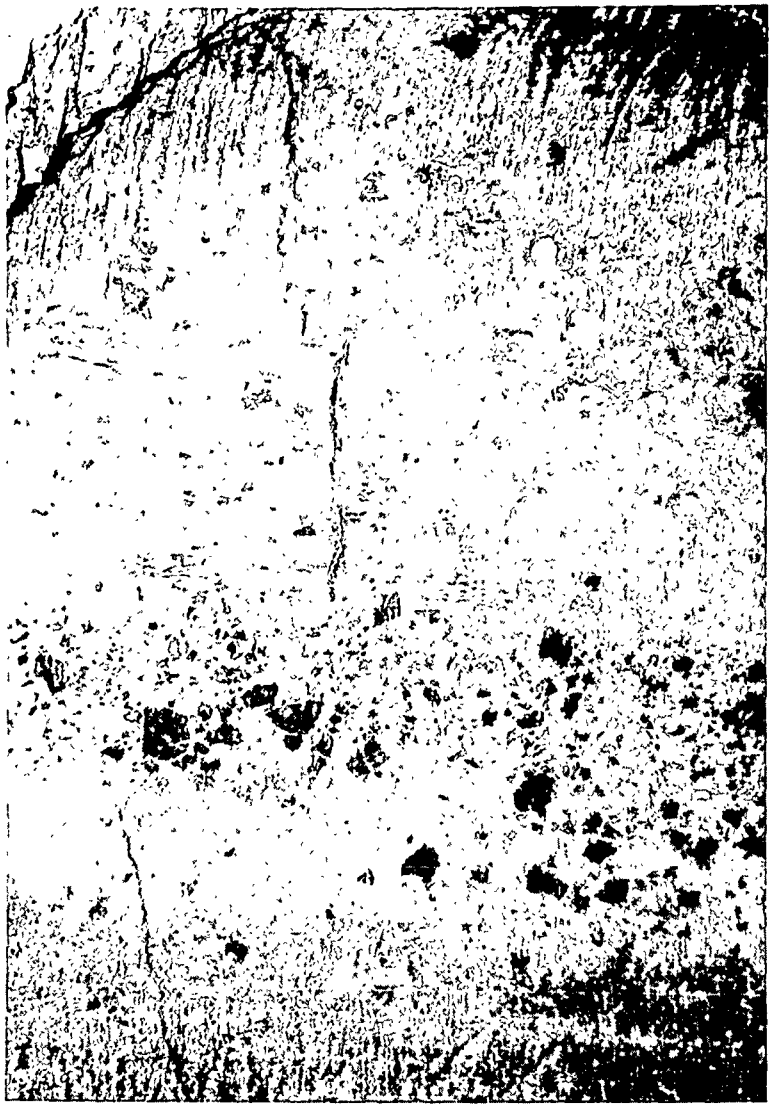

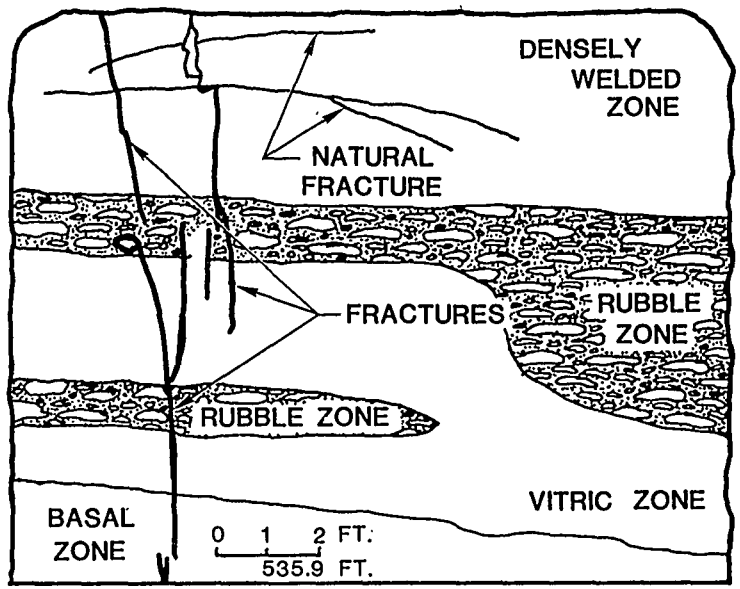

Figure 21. Photograph and Face Map at 535.9 ft in Mineback

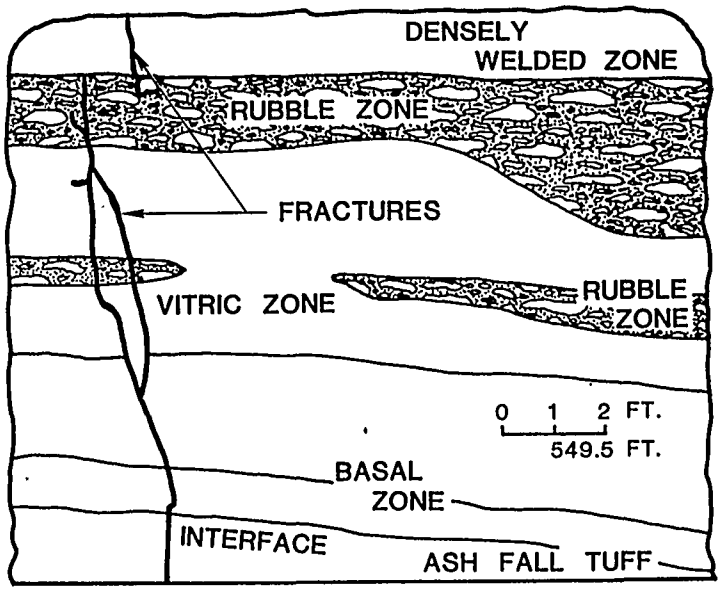

Figure 22. Photograph and Face Map at 549.5 ft in Mineback

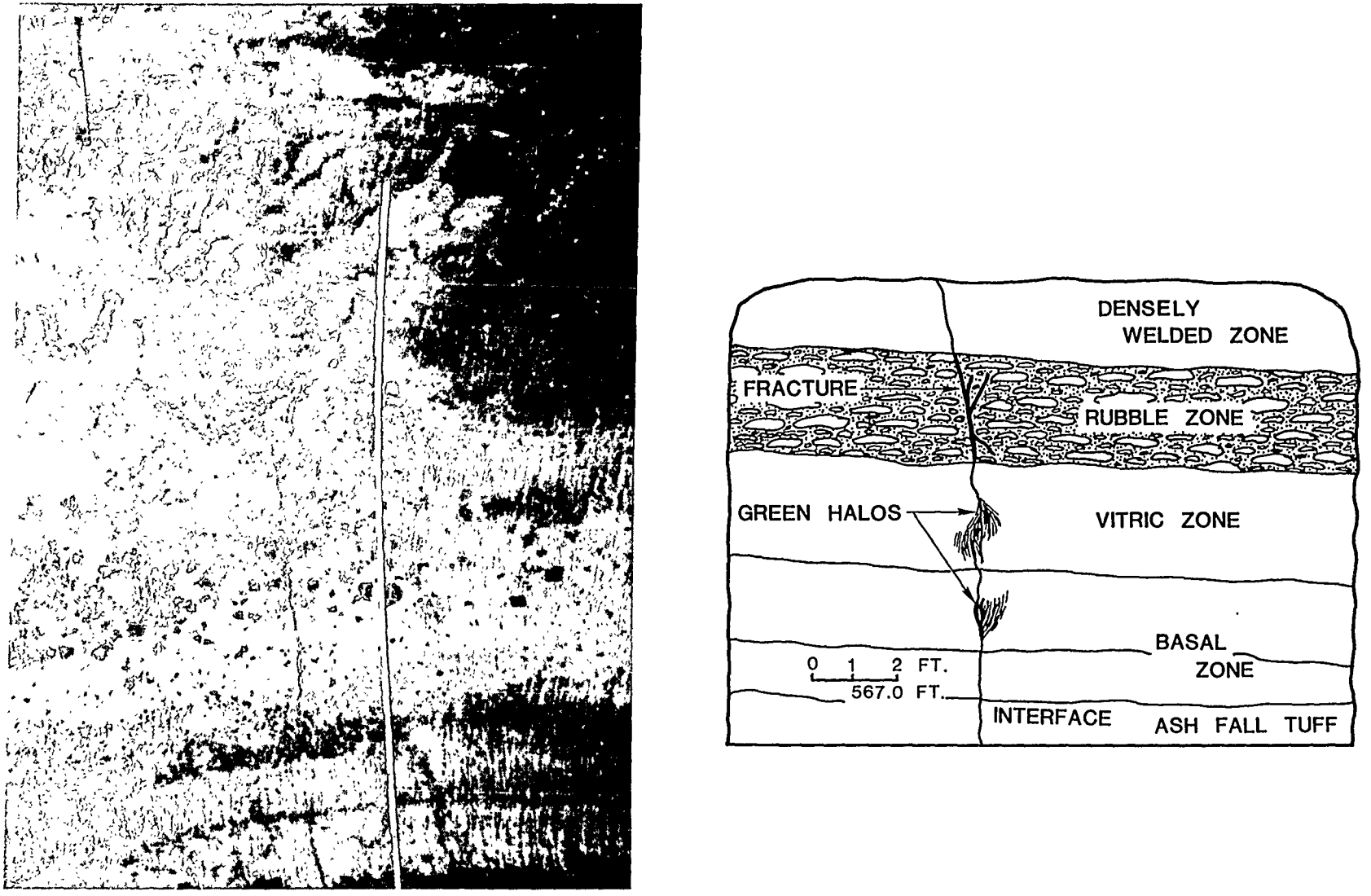

Figure 23. Photograph and Face Map at 567.0 ft in Mineback

locations in the center of the photo, the green grout is seen coating some natural cross fractures with a green halo. The fracture is approximately vertical here.

After the mineback along the interface was completed, a mineback raise was conducted at the borehole, using drilling and blasting techniques, to observe the fracture behavior near the borehole in the densely welded tuff. The raise was constructed through the elevation where the upper fracture was initiated. Figure 24 shows the raise at the 6225.1 elevation or 21.5 ft above the mineback grade. This point is just below the open-hole zone where the upper fracture was initiated. It is clear that the natural fracture system has a large effect on the hydraulic fracture by offsetting fracture growth. In many locations in the welded tuff the distance that the fractures travel along natural fracture planes is roughly the same as the distance they propagate through competent rock. Undoubtedly, a large percentage of the grout was lost into these natural fractures throughout the entire welded tuff zone. It appears that all of the grout at this location is black and green even though the blue (or gray) fracture was initiated just above this location. Generally, fracture widths are 3-7 mm. The fracture again intersects the borehole off center so it is possible that it never intersected the original 4 in borehole at this point.

The invert was also lowered a few feet to reveal the borehole near the location where the lower fracture was initiated. This is shown in Figure 25. At this point the hole diameter is six inches (recall that the hole was reamed to recover lost tools after the first fracture). A single fracture, greater than 10 mm in width originates from the NE side of the borehole. A number of strands initiate simultaneously from the other side of the borehole and coalesce into a main fracture and a secondary strand.

A plan view of the entire mineback is shown in Figure 26. The variation in the dip and strike of the fracture over the 150 ft length

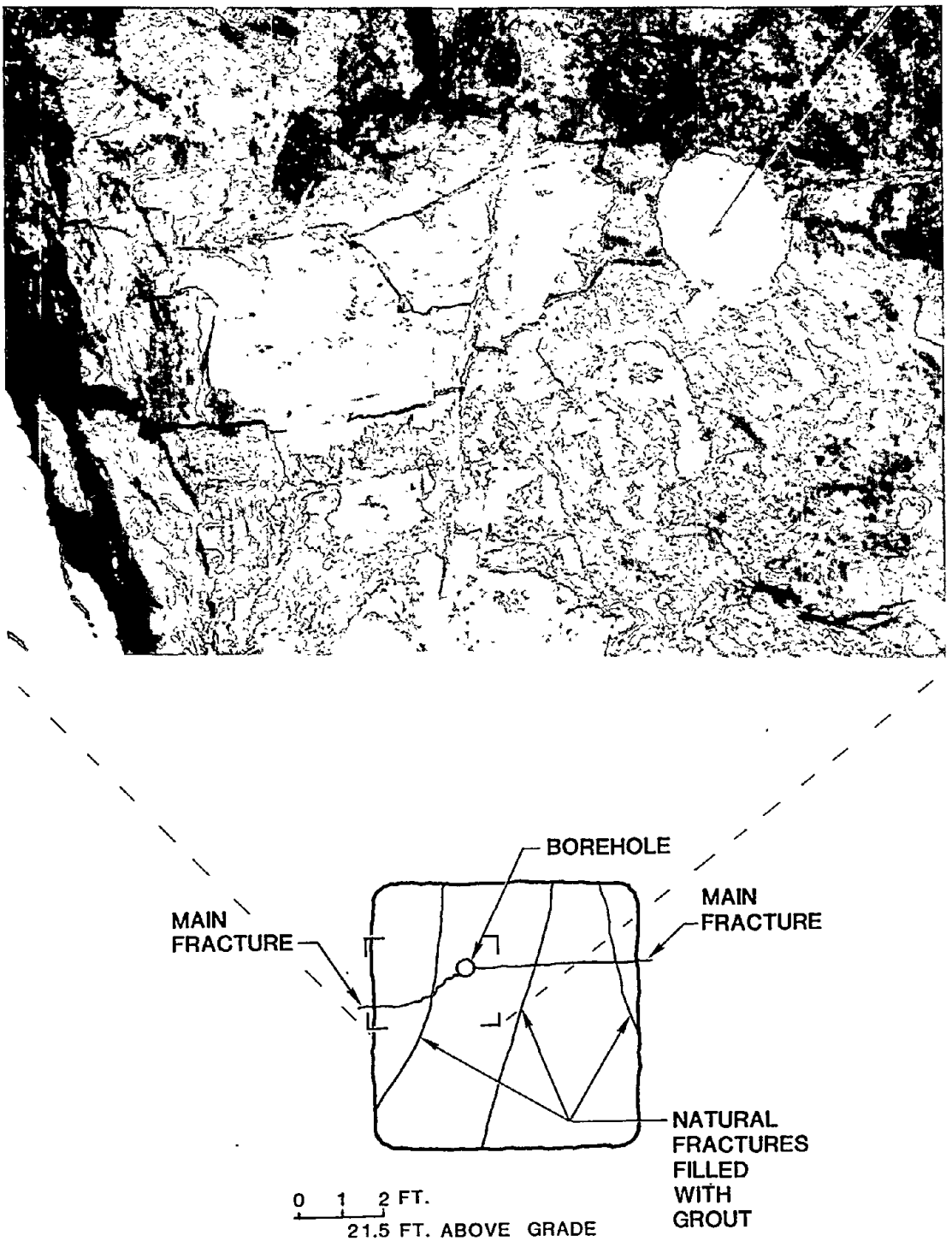

Figure 24. Photograph and Face Map of Raise at 21.5 ft Above Grade

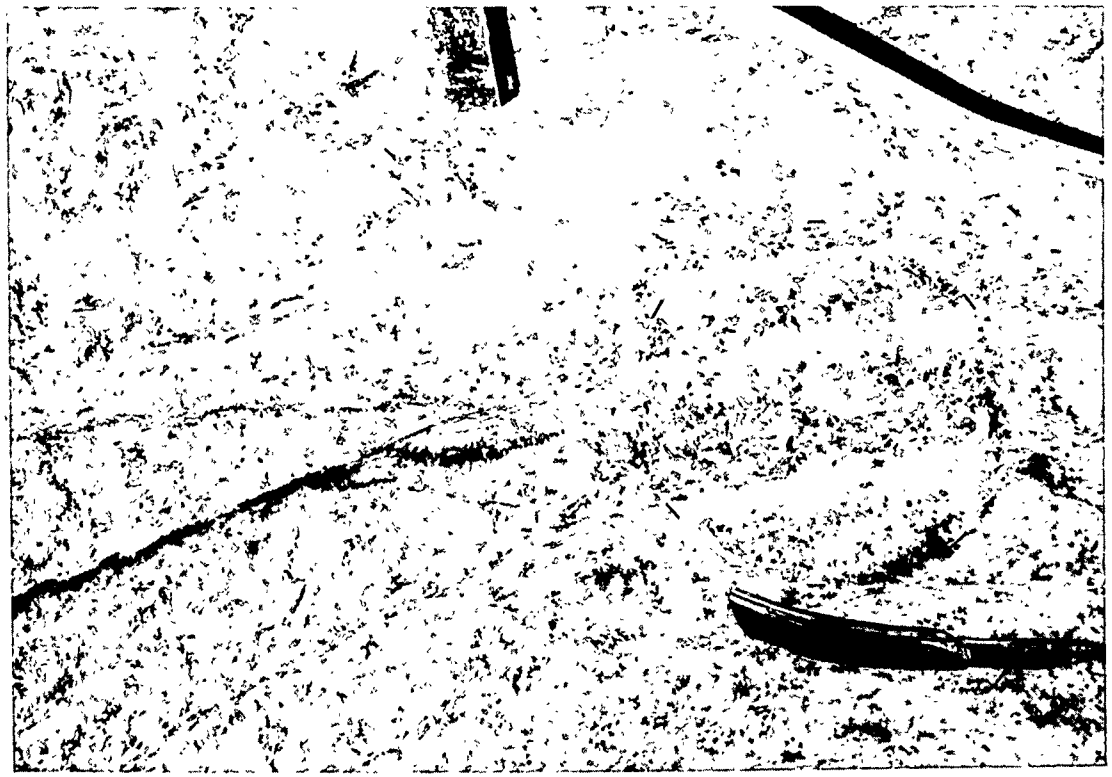

Figure 25. Photograph of Fracture Initiating from Borehole in Ash-Fall Tuff

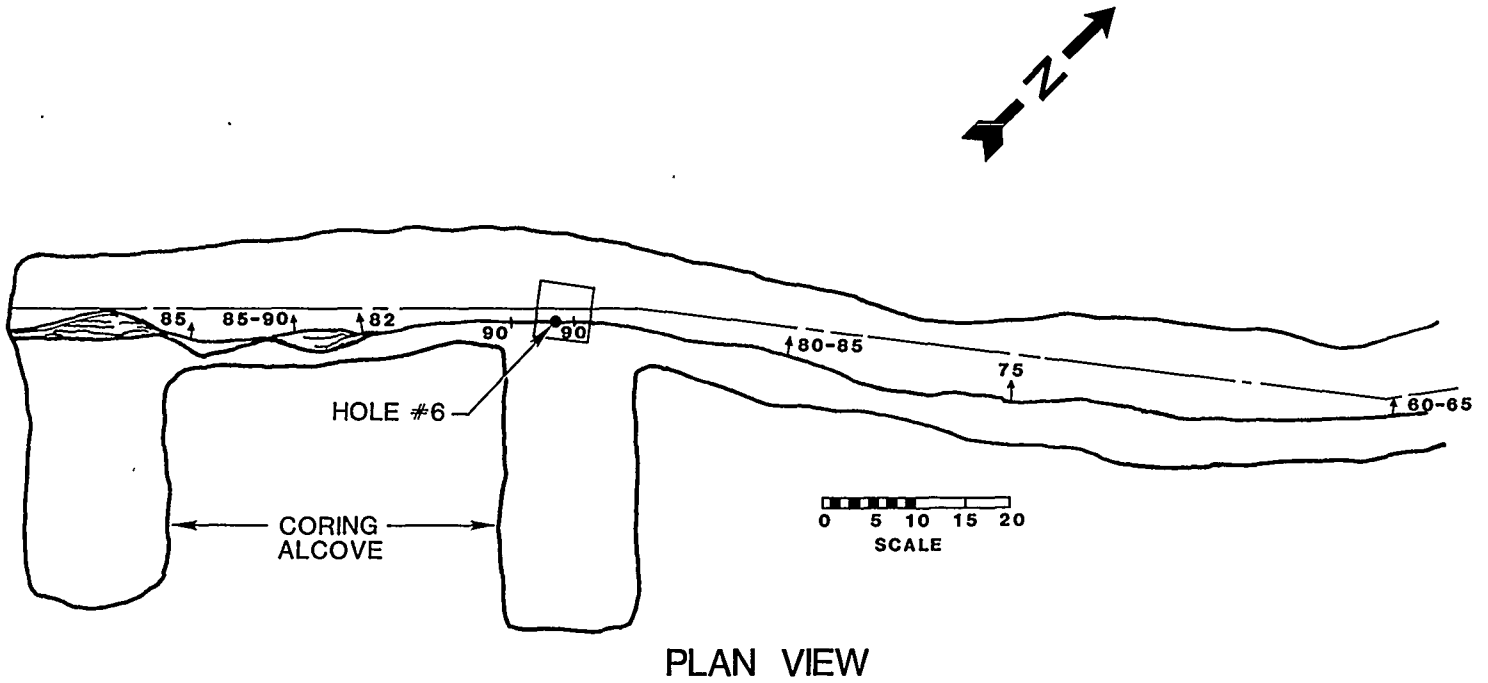

Figure 26. Plan View of Mineback of Fractures

is shown in the plan view. The average trend of the fractures (N53°E) is consistent with the direction of the maximum principal stress typically observed in G-tunnel. The two drifts to the SE of the fractures were excavated for future coring to locate the extent of the fracture above and below the mined region. A longitudinal cross-section of the mineback region is shown in Figure 27 along with the stratigraphy and the location of the borehole. Fractures were observed everywhere in this mineback area except the far left-hand top corner where it had pinched out.

The total width of the fractures (green, black and gray) at various locations along the mineback in the ash-fall tuff is shown in Figure 28. The width of only the green and black fracture along the mineback is shown in Figure 29. Although the fracture is plainly wider in the center and thins sharply near the tips, there are large variations in the center, particularly on the short wing. In determining the width, the sum of the strands at any location was used and this may account for the discrepancy. However, it was felt this was necessary because the main frac was often thinner when there were several secondary strands.

EXPLORATORY CORING RESULTS

In order to understand the behavior of a fracture at one point, say the interface, it is certainly helpful and may be necessary to understand it in the context of the entire fracture, its growth characteristics and overall geometry. Since it is only feasible to mineback a small percentage of a fracture this size (<5%), an exploratory coring program was started to locate the fracture at many locations remote from the mineback. The number of strands, thickness of the fracture, fracture orientation relative to the core and the color of the grout were determined at the core intercepts so that estimates of fracture extent and width contours could be made.

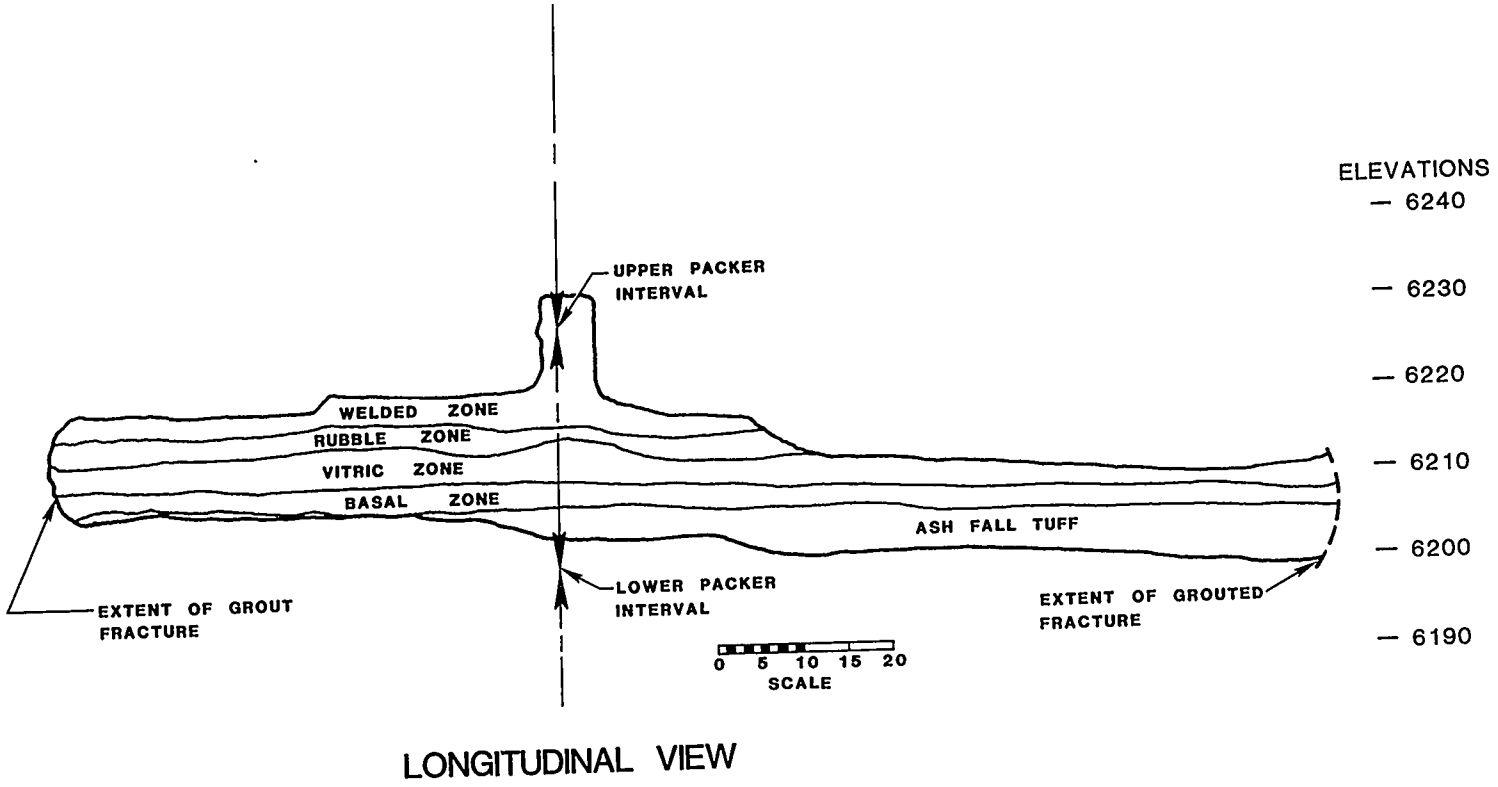

Figure 27. Side View of Mineback

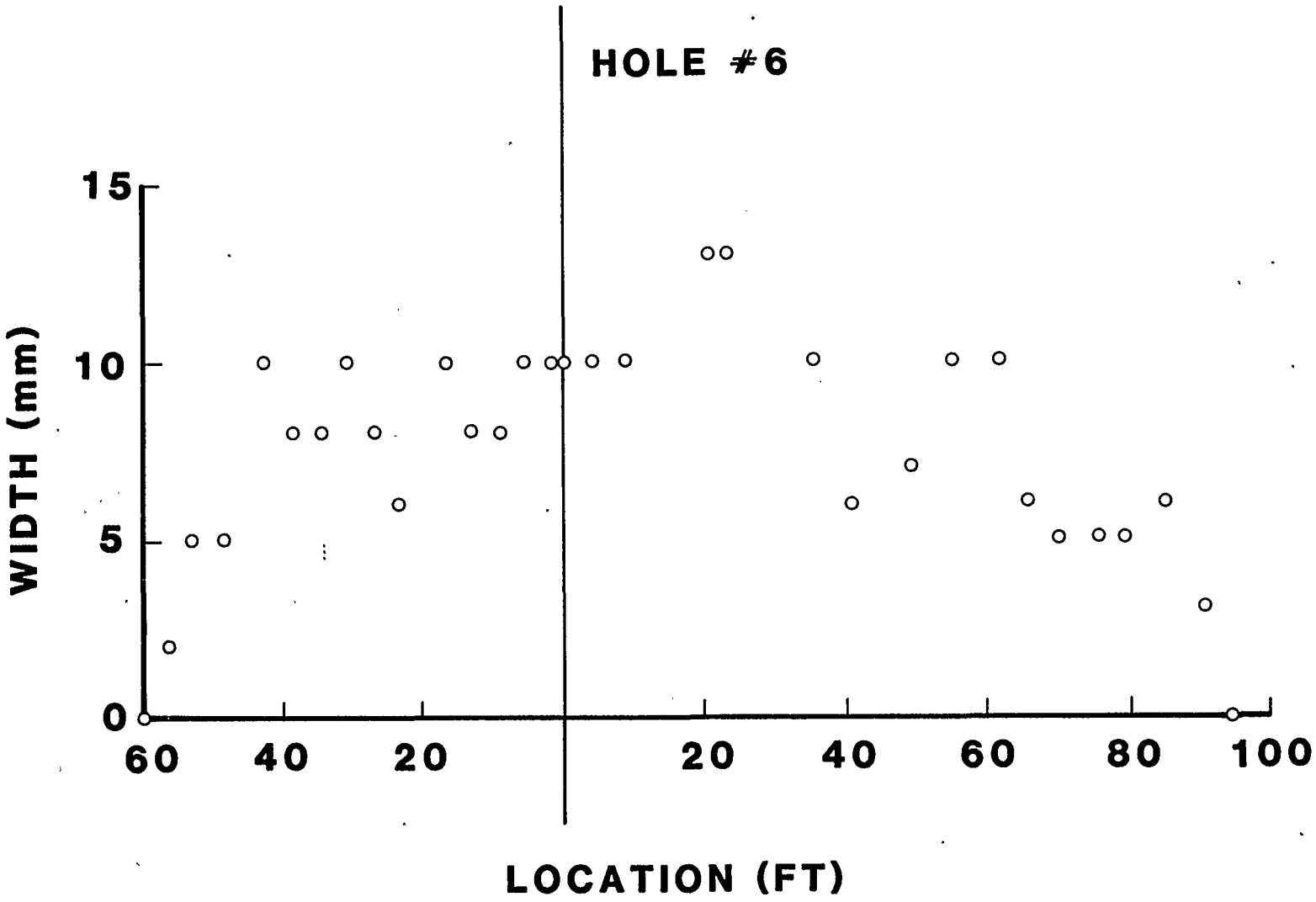

Figure 28. Width Measurements of Combined Grout Fractures

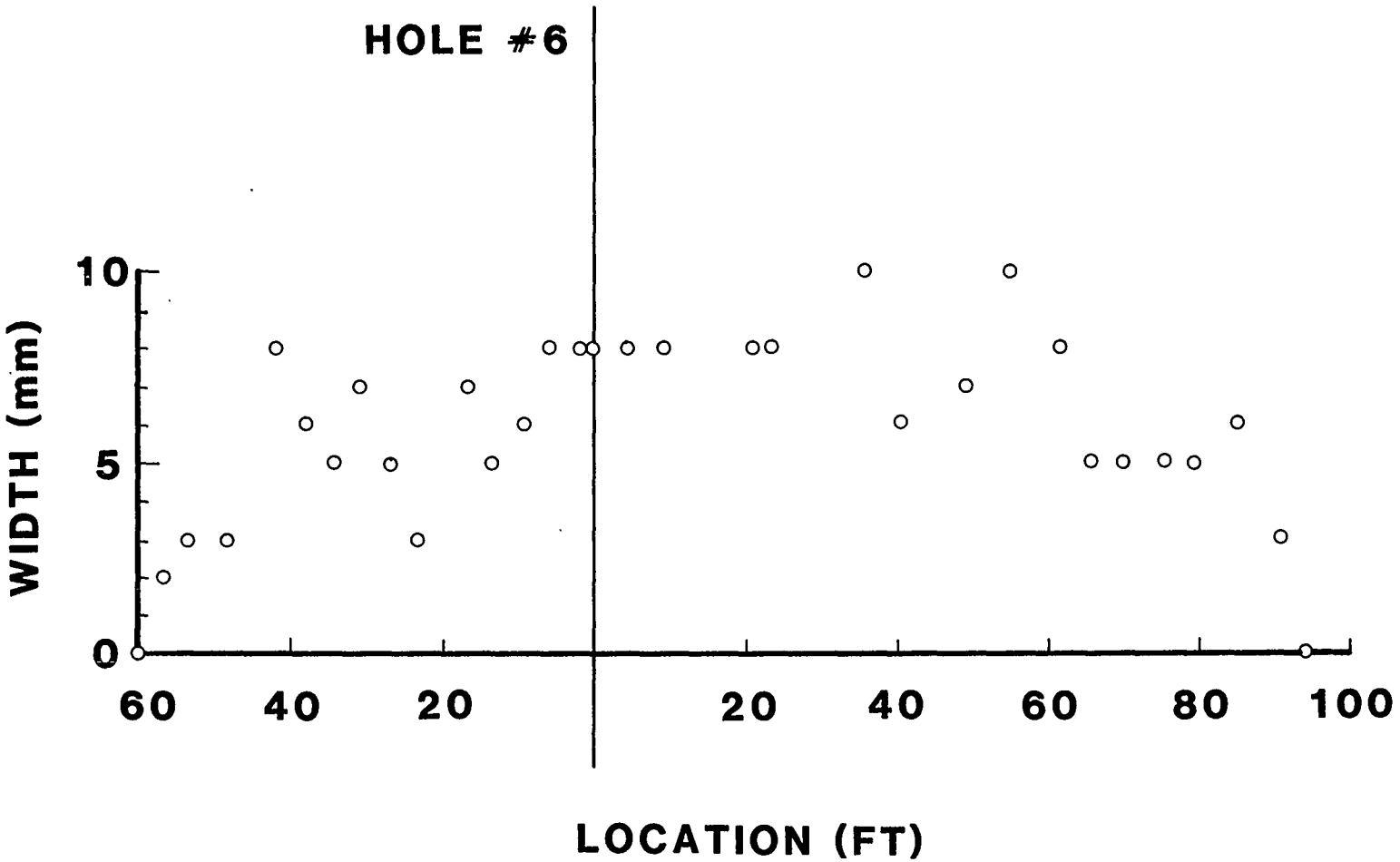

Figure 29. Width Measurements of Green and Black Grout Fracture

A total of 29 exploratory core holes were drilled intermittently, as other tunnel experiment commitments allowed, between August, 1978 and March, 1980. Figure 30 shows a side view of the exploratory coring results with respect to the mineback region. These results show where one or both of the fractures was intercepted by the core hole. Intercept locations, fracture widths and grout colors are given in Table 4. The green and black grout are combined for the width data because it was difficult to separate them due to mixing. From this data it was found that the green and black fracture was limited to a region from about 50 ft below the interface to the top of the combined fractures. Only gray grout was found farther than about 50 ft below the interface and almost none above. This is shown in Figures 31 and 32 which show width contours for the combined fractures and for the green and black fracture respectively. As seen in Figure 32, the green and black fracture, which was conducted first, is essentially a penny-shaped fracture and is not affected by the high modulus layer above. On the other hand, most of the gray grout was forced downward into the ash-fall tuff far below the interface even though this fracture was initiated in the welded tuff. The width contours shown in Figures 31 and 32, as well as the indicated fracture boundaries should not be considered rigorous since there are not very many data points except through the mineback section, A-A'. This is obvious when one compares the steep gradients at the tips along A-A' compared to the relatively slow narrowing elsewhere. This is a result of the smoothing of the contour routine. Again, fracture widths given here are for the sum of all strands. The fracture width observed at the wellbore is consistent with that calculated by the design codes.

One problem with these results is that they account for about 40% and 60% of the first (green and black) and second (gray) injected volumes respectively. It is expected that 20-30% of this loss can be accounted for by water loss from the grout slurry both during and after fracturing.

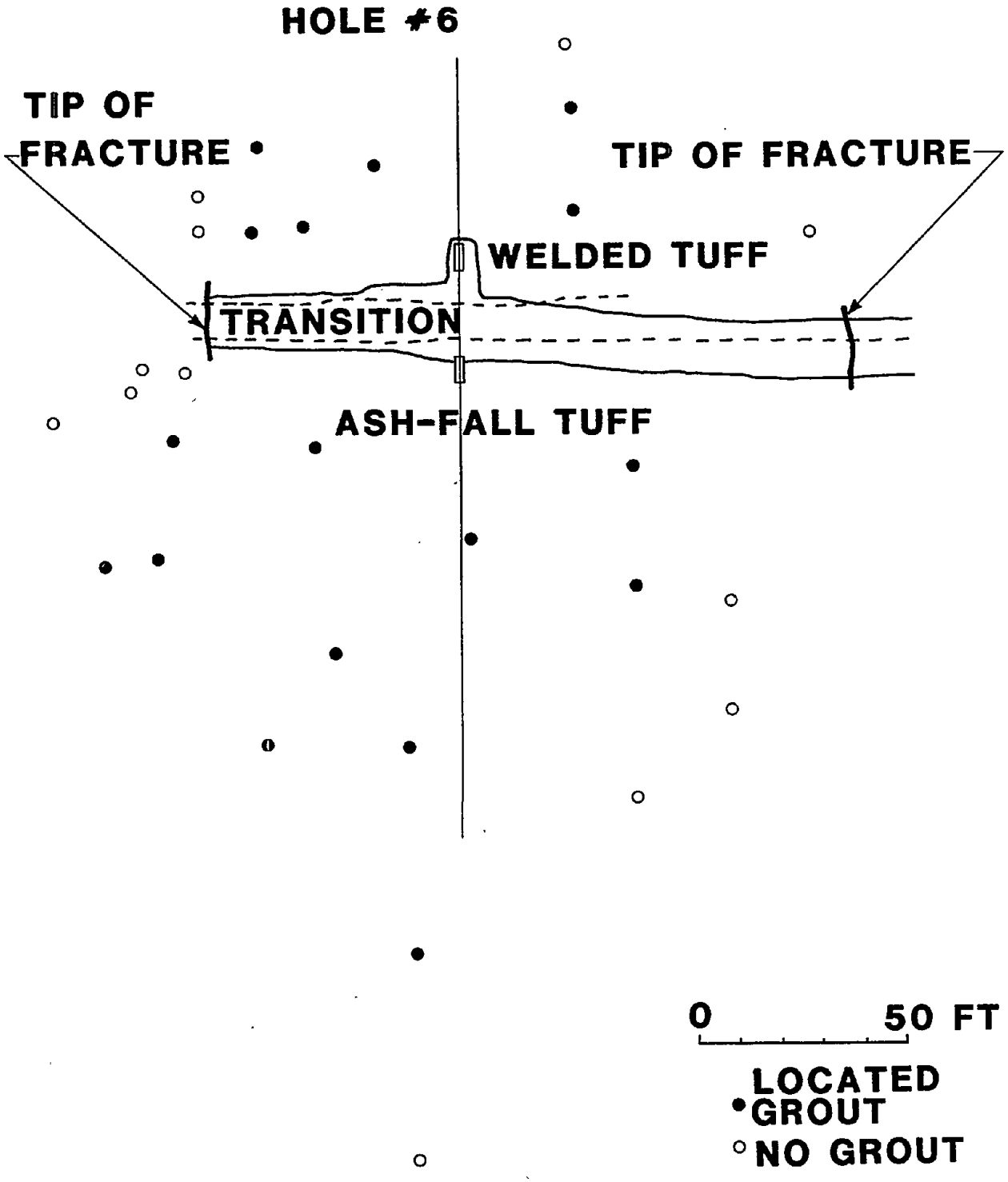

Figure 30. Side View of Results of Exploratory Coring Program

TABLE 4

Exploratory Coreholes

HOLE	GROUT INTERCEPTS (ft)	COLOR	THICKNESS (mm)		POSITION FROM HOLE #6 (ft)	POSITION FROM MINEBACK (ft)
EV6-4	11.7	Green & Black	2			
	25.5	Green & Black	4			
	43. (2)	Green & Black	2 & 6	*	19.5 SW	29 above back
	43.4	Green & Black	Trace			
	50.	Green	Trace			
EV6-5	16.	Green	3			
	21.	Green & Black	1.5			
	35.8	Green	1	*	36.5 SW	17 above back
	35.9	Black	1			
	36.2	Green	3			
EV6-6	30.6	Gray	4		66.5 SW	23 below invert
EV6-7	None				94.5 SW	19 below invert
EV6-8	None				76.5 SW	11.5 below invert
EV6-9	None				74. SW	5.5 below invert
EV6-10	None				63.5 SW	6 below invert
EV6-11	71.5 (2)	Gray	7 & 2	*	27. SW	74 below invert
	86.3	Gray	<1			

(Table 4 Continued) Exploratory Coreholes

HOLE	GROUT INTERCEPTS (ft)	COLOR	THICKNESS (mm)		POSITION FROM HOLE #6 (ft)			POSITION FROM HINEBACK (ft)	
EV6-12	84.5	Gray	Trace						
	95.7	Gray	3		*	43	SW	97	below invert
	100. (2)	Gray	2 & 1						
EV6-13	None					61	SW	24	above back
EV6-14	18.5	Green & Black	1.5						
	20-24	Green & Black	Pockets						
	41.	Green	1		*	47.5	SW	36	above back
	42.5	Green	1.5						
	47.5	Green	Trace						
EV6-15	6.7	Green	<1						
	8.9	Green	1						
	9-11	Green	Trace						
	11	Green	1		*	46.5	SW	19.5	above back
	21.3	Green	1						
	23.4	Green	<1						
	28.3-30.6	Green	2-8						
	30.7	Green	1						
EV6-16	None					61	SW	15	above back
EV6-17	57.7	Gray	5			69	SW	50.5	below invert

(Table 4 Continued) Exploratory Coreholes

HOLE	GROUT INTERCEPTS (ft)	COLOR	THICKNESS (mm)		POSITION FROM HOLE #6 (ft)		POSITION FROM HINEBACK (ft)	
EV6-18	65.4-66	Gray	<1	*	82.5	SW	56	below invert
	66.1	Gray	3					
EV6-19	None				97	SW	54.5	below invert
EV6-22	102	Gray	6		3.5	SW	95.5	below invert
EV6-23	147	Gray	7.5		5	SW	162.	below invert
EV6-24	None				6	SW	252.	below invert
EV6-25	None				46	NE	94	below invert
EV6-26	78.4	Green	1	*	46	NE	57	below invert
	78.7	Green	2					
EV6-27	39.9	Green & Black	4		27.5	NE	23	above back
EV6-28	59.9	Green & Black	2		27.5	NE	47	above back
EV6-29	None				27.5	NE	62	above back
EV6-30	None				84.5	NE	35	above back
EV6-31	None				66	NE	80	below invert
EV6-34	104.3	Green	1		79	NE	55.5	below invert
34 cont. EV6-35	52.9 (2)	Green & Gray	7 & 3		42	NE	23	below invert
EV6-36	57.9	Green & Gray	4 & 3		34	SW	28	below invert

*Where multiple fracture strands were intersected, only the position which is consistent with the overall fracture plane is given.

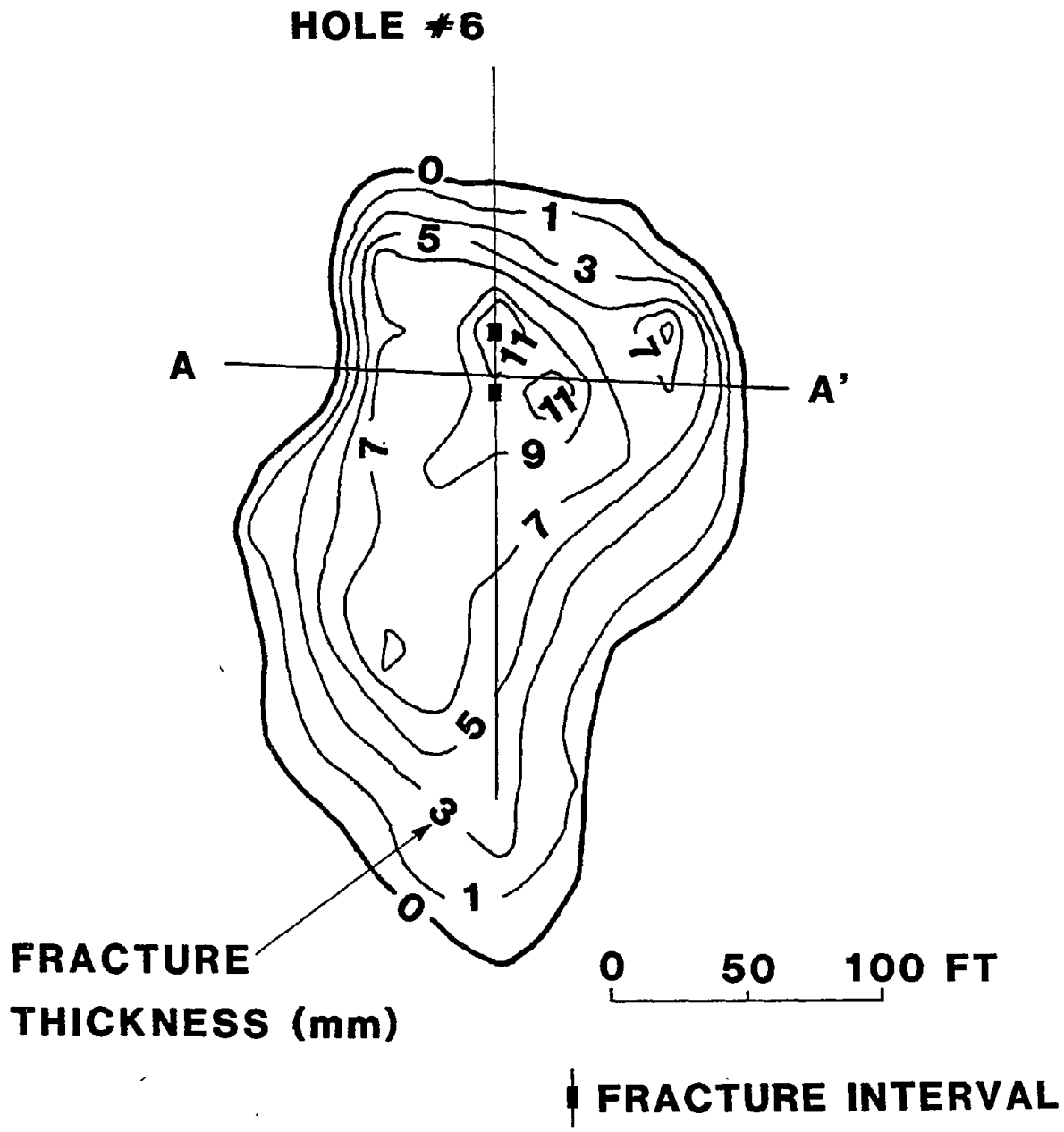

Figure 31. Side View Showing Width Contours of Combined Grout Fractures

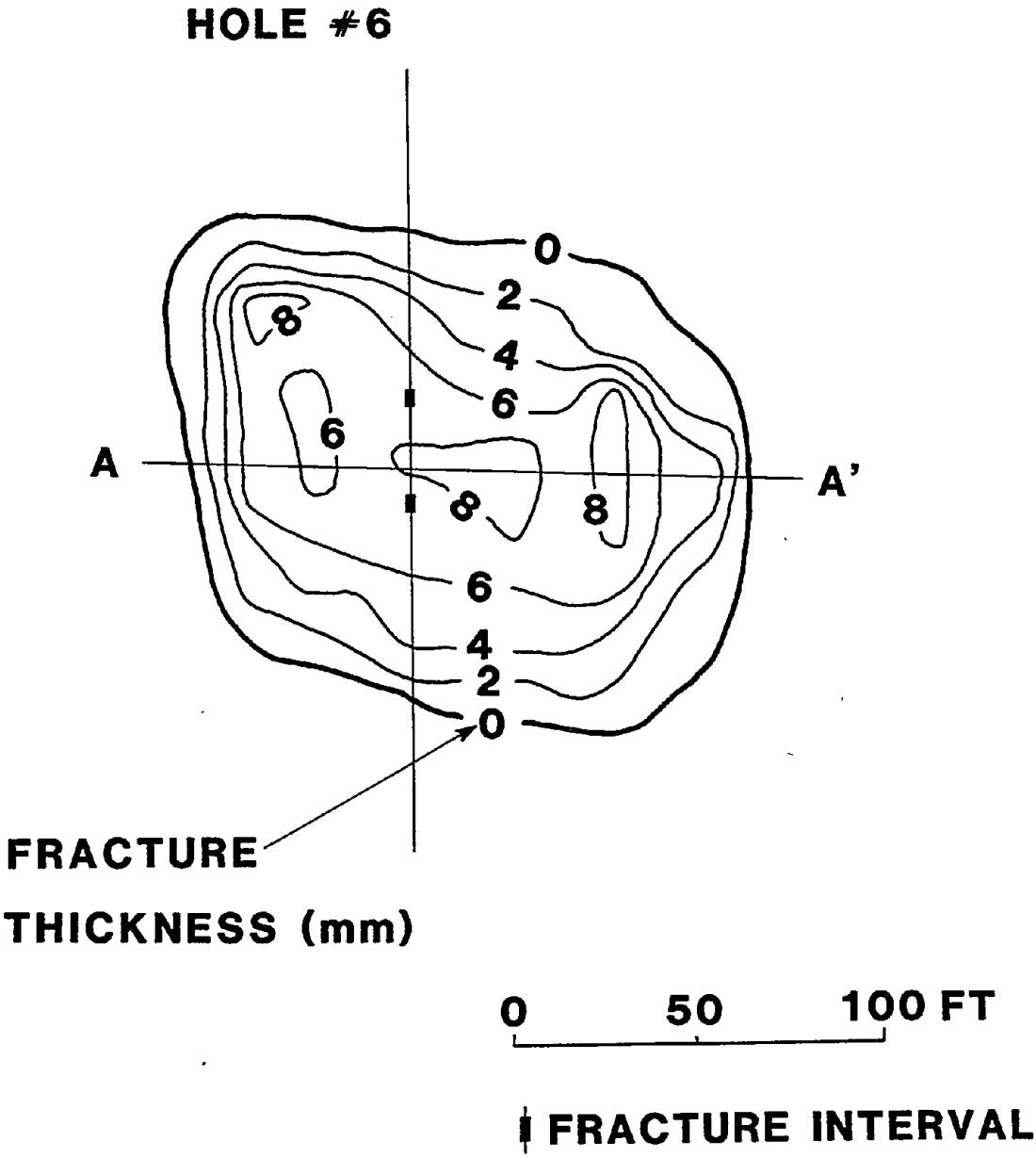

Figure 32. Side View Showing Width Contours of Green and Black Grout Fractures

However, 30-40% of the green and black fracture cannot be accounted for except as leakoff into natural fractures, mostly in the welded tuff. During mineback some evidence of this was seen in the welded tuff near the borehole. Further evidence can be gained from the results of the coring program as seen in the results in Table 4. Up in the welded tuff, coreholes EV6-4, 5, 14 and 15 show several intercepts of green or black grout. These are plotted in Figure 33 in plan view and cross section. It appears from these data, together with mineback information, that the numerous strands are due to the extensive natural fracture system. Apparently the fracture would intercept a nearly perpendicular natural fracture, follow it for as much as 10 to 20 ft, and then initiate several more strands (possibly in other perpendicular natural fractures) which in turn will intercept other natural fractures. In this way an extensive network of grout filled fractures exists in the welded tuff and this may account for the remaining cement.

It is interesting to note that wherever the two fractures were found in the same region, they were usually side by side. Apparently the gray fracture, which was initiated in the high modulus welded tuff, essentially propagated alongside the first fracture. Results of the first fracture are valid; results from the second are obscured. Thus little useful information was obtained for fracture behavior at an interface should the fracture approach a low modulus material from a high modulus material.

IN SITU STRESS MEASUREMENTS

Two different sets of in situ stress data were obtained to determine what affect the stresses may have had on fracture behavior. In situ stress measurements are made using small volume hydraulic fractures[28] (minifracs) to provide an instantaneous shut-in pressure (ISIP) which is equivalent to the minimum principle in situ stress. These are conducted by isolating a short section of an open hole with straddle packers,

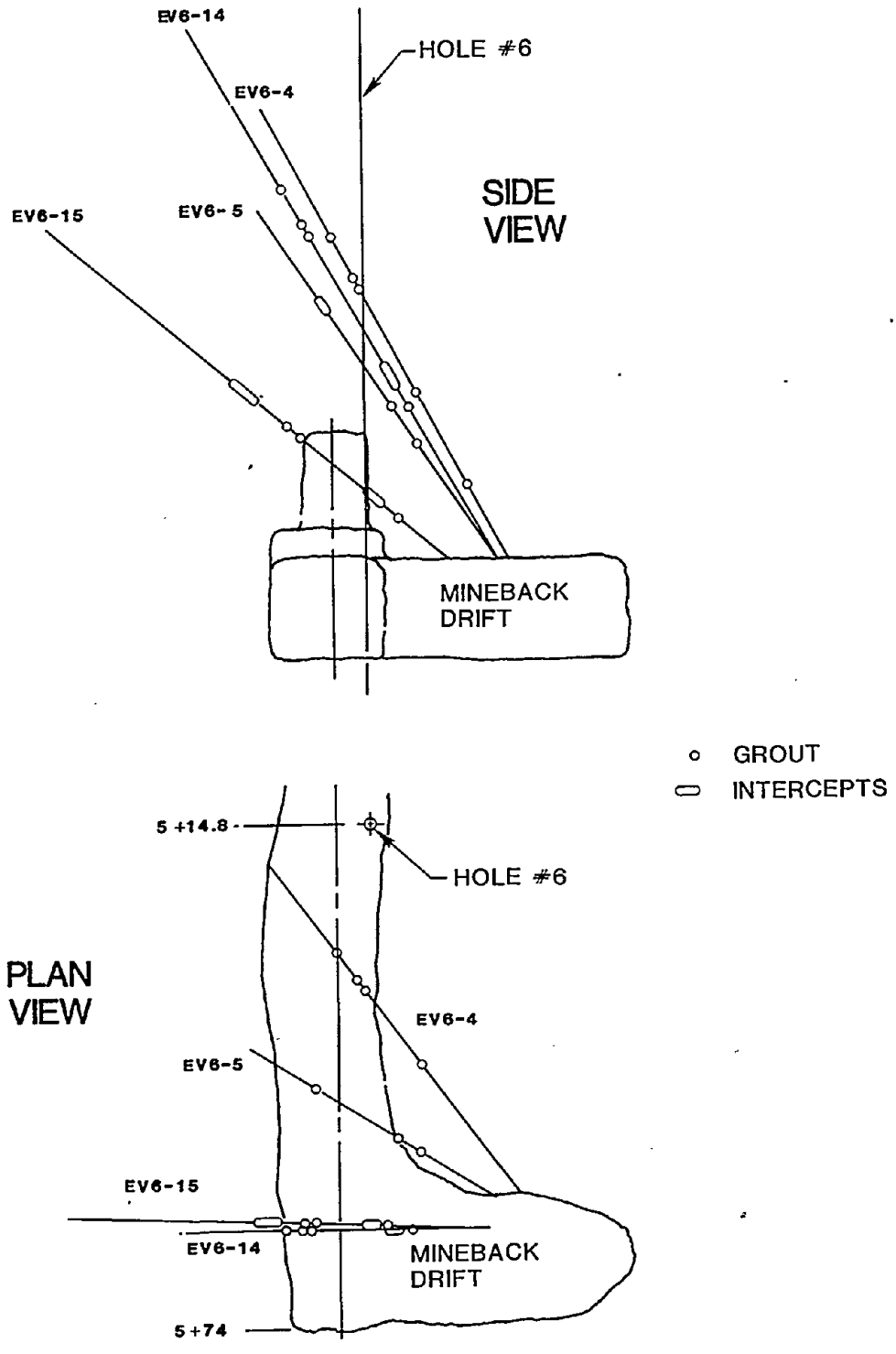

Figure 33. Multiple Fracture Strands in Welded Tuff as Determined by Exploratory Coring Program

pumping a small volume of water to break down the formation, and shutting the zone in to obtain the pressure decline. Accuracy is usually ±20 psi although in different areas the accuracy may vary considerably.

The first stress measurements were conducted in November 1977 before the mineback reached the fractures. Three coreholes were drilled from a point about 200 ft from the borehole to attempt to locate the grout fractures so the mineback could proceed in the most direct way. Afterwards, minifracs were conducted in several zones of two holes as shown in Figure 34, to determine the horizontal distribution of stress in this region. The data from EV6-1 and EV6-2, which were essentially horizontal in the ash-fall tuff, are given in Figure 34 and in Table 5. The stress distribution along EV6-1 is plotted in Figure 35 and it can be seen that there is a definite structure to the stress magnitude. What is interesting about this is that the location of the Hole #6 fracture is at the minimum of one of these structures. Although the fracture does not intercept EV6-2, a projection of the fracture direction would also intersect a minimum point as shown in Figure 36. What this indicates is, that not only does the fracture propagate perpendicular to the minimum principal in situ stress, but it also follows any minimum in the contours of the minimum principal in situ stress. In short, it follows the path of least resistance even with respect to variations in the minimum stress.

No breakdowns were seen in any of the 22 zones conducted in these two holes, yet the core from these holes showed that the rock was very competent with few, if any, fractures. From the orientation of the induced fractures, it is known that these two nearly horizontal coreholes are closely aligned with the maximum principal stress direction. To determine the stress concentration at the borehole for this geometry, the two principal stresses acting perpendicular to the borehole axis are the minimum principal horizontal in situ stress which is 350 psi and the overburden stress which is 1300 psi. One can see then that

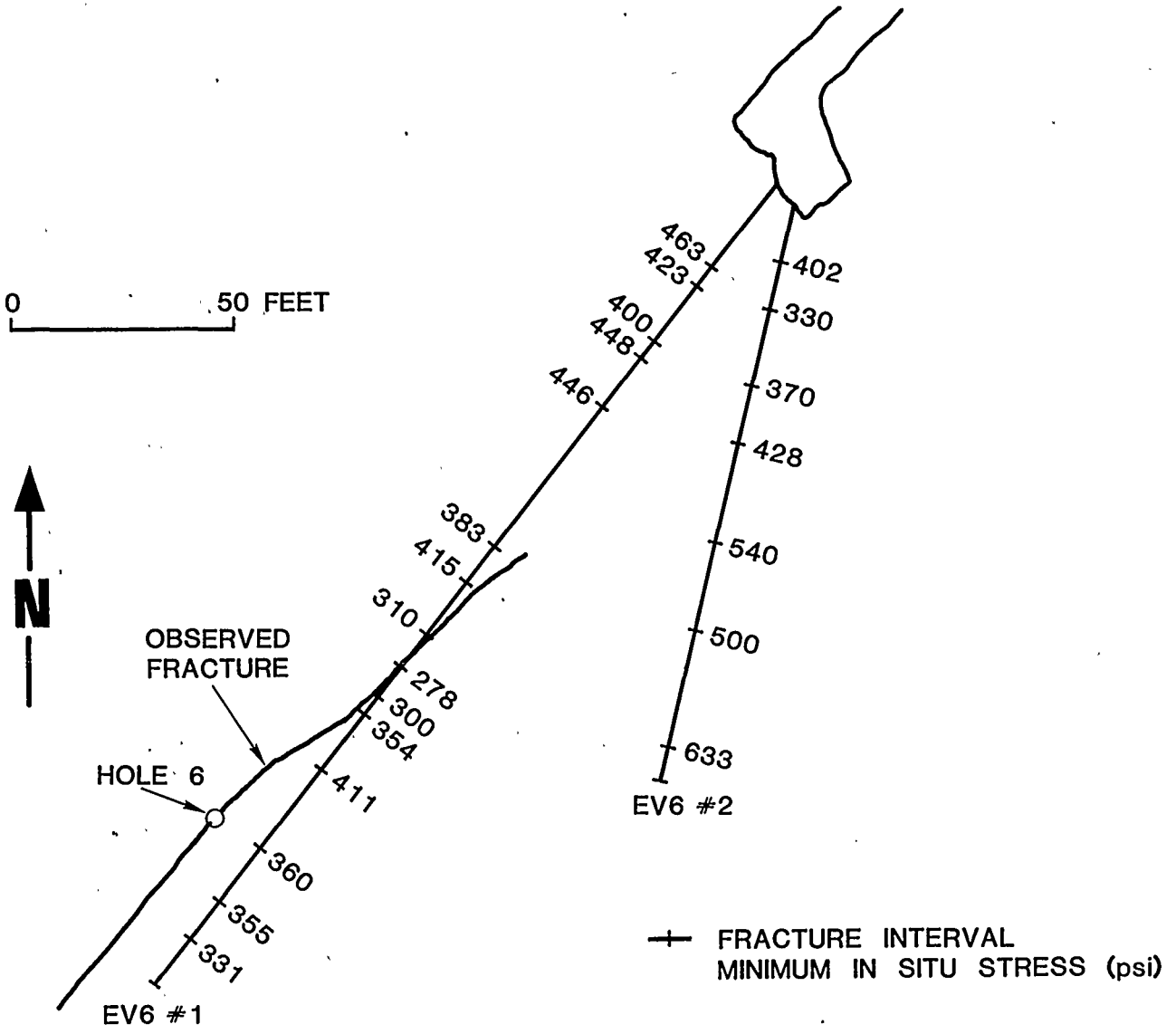

Figure 34. Results of In Situ Stress Measurements in EV6 #1 and EV6 #2 Conducted Before Mineback

TABLE 5

In Situ Stress Data: EV6-1 and EV6-2

HOLE	DEPTH (ft)	# OF PUMPS	AVG VOLUME (gal)	P_c (PSI)	P_f (PSI)	ISIP (PSI)
EV6-1	214	4	6	-	425	331
	204	4	7	-	440	355
	189	2	6.5	-	430	360
	167	4	7	-	500	411
	151	4	8	-	630	354
	146.5	4	6	-	390	300
	138	2	5.5	-	320	278
	129	2	4.5	-	395	310
	114	2	7	-	520	415
	104	2	6	-	450	383
	64	5	8	-	520	466
	50	2	7.5	-	555	448
	45	2	6	-	465	400
	29	4	5	-	500	423
	24	2	6	-	525	463
EV6-2	124	2	4	-	900	633
	98	2	7	-	780	500
	78	2	5	-	880	540
	55	2	5	-	685	428
	42	2	3.2	-	570	370
	24.5	2	3.3	-	445	330
	13	2	3	-	525	403

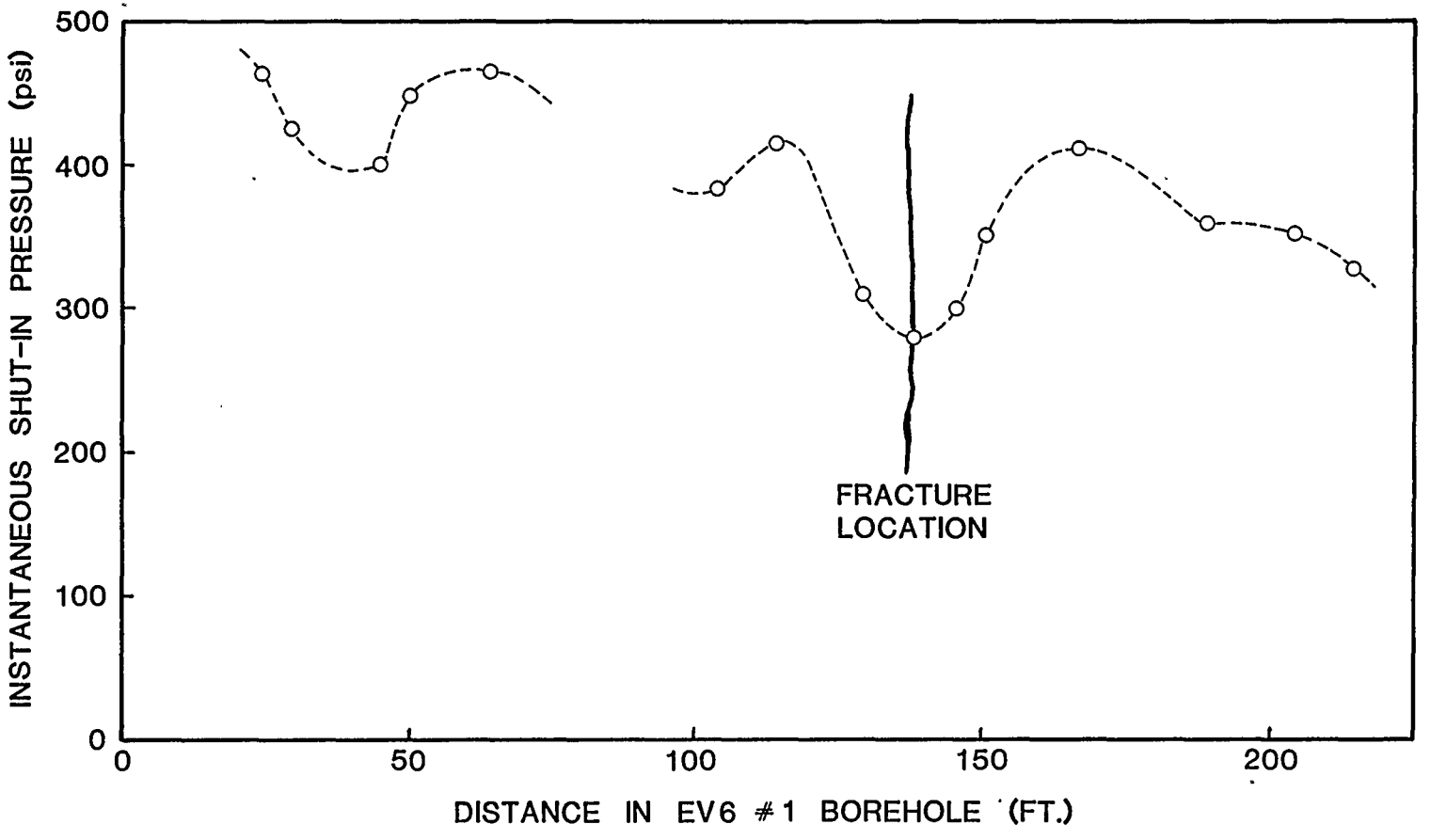

Figure 35. Location of Fracture with Respect to Distribution of the Minimum Principal In Situ Stress in EV6 #1

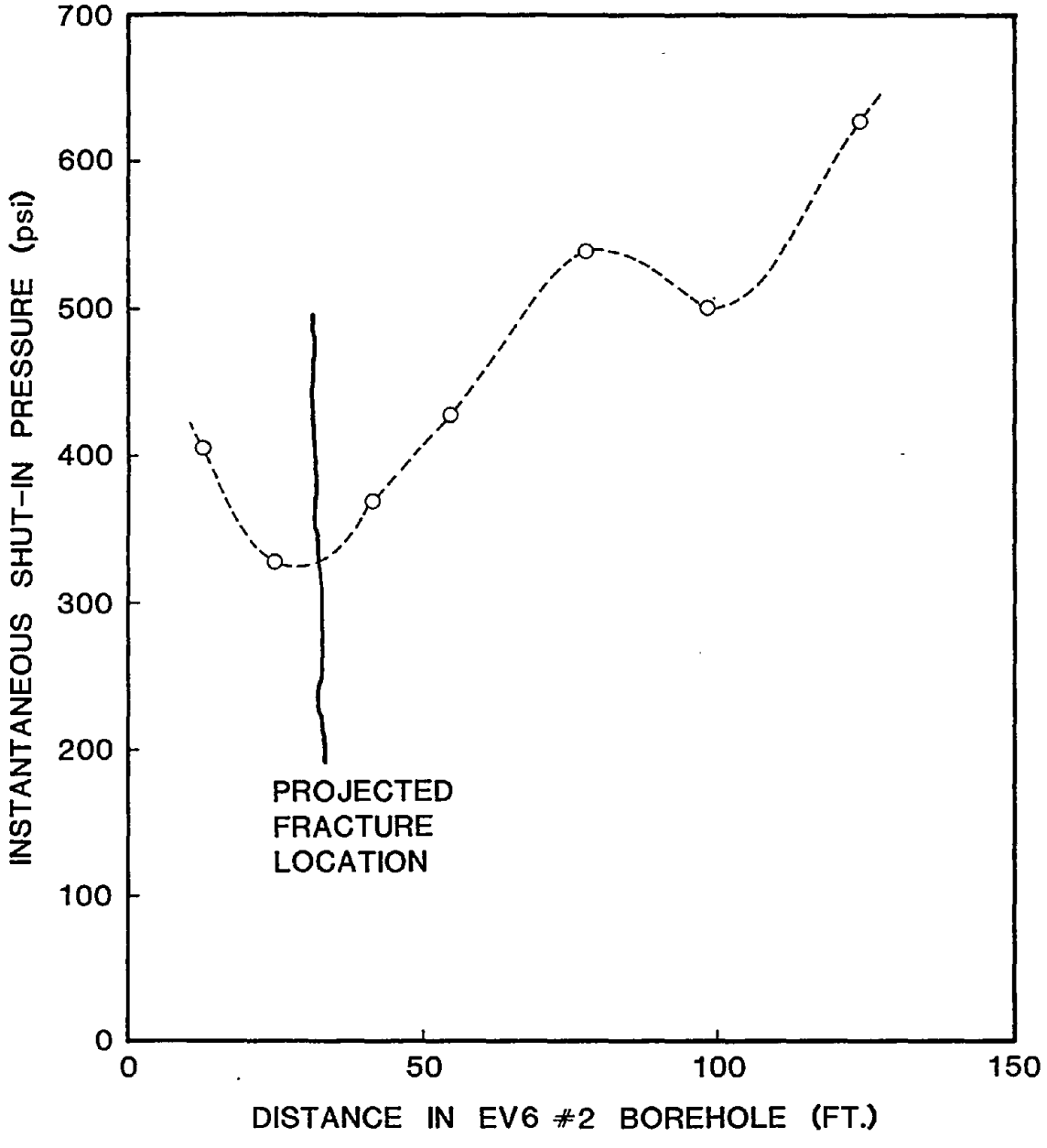

Figure 36. Projected Fracture Intercept in EV 6 #2 with Respect to the Distribution of the Minimum Principal In Situ Stress

the minimum compressive stress at the borehole wall, which is $3\sigma_{min} - \sigma_{max}$, is -250 psi, which is tension. For this weak material the borehole has probably broken down just by drilling the borehole. At worst it would require another 200-300 psi more to break down the most competent tuff and this is still below the minimum principal in situ stress. Thus, one should not expect to see any breakdown with this combination of stresses and hole alignment.

No data is shown from EV6-3 because this hole was drilled upward into the welded tuff at +7° and many difficulties were encountered attempting to fracture this rock. Some data, which were obtained in three zones, were difficult to interpret and no reasonably accurate measurements could be made. However, it did appear that the ISIPs or the minimum principal in situ stresses were exceptionally low; they were probably less than 200 psi and possibly less than 100 psi.

A detailed study of the vertical distribution of the in situ stresses was made in September 1980. Two of the exploratory coreholes, EV6-24 which was drilled 81° down to a TD of 302 ft and EV6-29, which was drilled 58° up to a TD of 150 ft., were fractured in several zones, each using the standard minifrac technique. Essentially these measurements were made along the Hole #6 borehole although EV6-29 does deviate somewhat to the NW. The ISIP or minimum principal in situ stress data is shown in Figure 37 and Table 6. It can be seen that there are large and quite rapid changes of stresses throughout the 350 ft of section studied. Also, the stress in the densely welded tuff is quite low.

This distribution of stresses can be explained qualitatively if one considers the mesa in its present condition and forgets for the moment its geologic history. Essentially, the mesa consists of tens or even hundreds of ash-fall tuff layers of varying thickness and properties with two thin, high-modulus, welded tuff strata at widely separated locations. At the present point in geologic time, the layers are stacked, well-bonded and predominantly gravity-loaded. This results in a com-

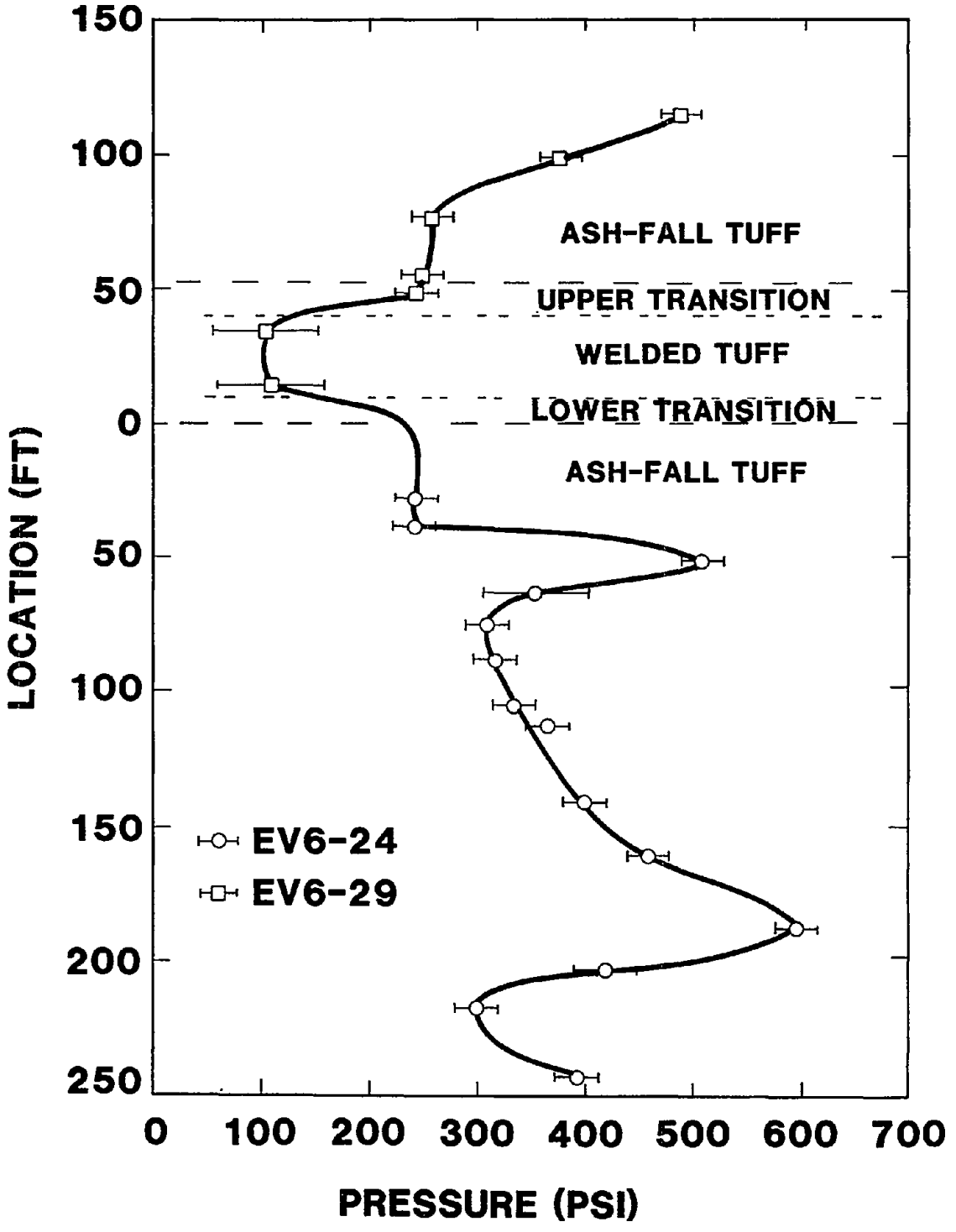

Figure 37. Minimum Principal In Situ Stress Distribution Throughout the Hole #6 Fracture Region

TABLE 6

In Situ Stress Data: Ev6-24 and EV6-29

HOLE	DEPTH (ft)	DISTANCE FROM INTERFACE (ft)	BREAKDOWN P_c (PSI)	BREAKDOWN P_f (PSI)	BREAKDOWN ISIP (PSI)	BREAKDOWN VOLUME (gal)	REPUMP P_f (PSI)	REPUMP ISIP (PSI)	REPUMP VOLUME (gal)
EV6-24	233	- 244	610	450	390	2.1	430	420	1.3
	207	- 218	527	330	300	2.1	325	310	1.6
	192	- 204	845	685	420	2.2	670	450	1.8
	165	- 187	871	670	595	1.8	630	560	1.9
	150	- 162	915	480	460	2.3	470	460	1.4
	130	- 142	695	420	400	2.4	405	380	1.7
	110	- 113	987	430	365	2.3	410	360	1.7
	92	- 105	465	350	335	2.3	340	320	1.6
	75	- 88	413	333	315	2.0	333	300	1.4
	62	- 75	450	330	310	1.9	330	280	1.8
	50	- 63	471	365	355	2.1	360	310	1.3
	38	- 52	753	575	510	2.1	555	500	1.8
	25	- 39	509	290	240	2.3	280	240	1.5
	14	- 28	408	325	240	1.6	315	240	1.3

TABLE 6 (Continued)

In Situ Stress Data: Ev6-24 and EV6-29

HOLE	DEPTH (ft)	DISTANCE FROM INTERFACE (ft)	P_c (PSI)	BREAKDOWN P_f (PSI)	ISIP (PSI)	VOLUME (gal)	REPUMP P_f (PSI)	ISIP (PSI)	VOLUME (gal)
EV6-29	134	+ 114	694	540	490	2.4	555	485	1.2
	115	+ 98	560	400	380	2.2	400	-	1.5
	90	+ 76	358	280	260	2.3	280	260	2.1
	65	+ 55	508	280	250	1.8	260	250	1.5
	56	+ 47	328	275	245	1.9	280	245	1.5
	40	+ 34	-	400	105	2.2	430	110	1.3
	16	+ 14	-	590	110	2.5	620	100	1.3

pressional loading of the layers and effectively tries to squeeze the tuffs out the sides of the mesa. The ash-fall tuff, which has a very low Young's modulus and a high Poisson's ratio is squeezed out much farther than higher modulus rocks. Since the strata are well bonded, the ash-fall tuff drags the narrow welded tuff layer out with it resulting in a decreased compressional state or even tensional state of stress in the high modulus, low Poisson's ratio, welded tuff. This also explains why the welded tuff is so uniformly fractured. Of course, the geologic history, such as cooling phenomena of the tuffs, erosional relief of the mesa, alteration, and other factors will affect the local structure of the stresses and specific magnitudes and orientations. Also, factors such as creep and the limited effect of tectonics may have affected the stress state in the welded tuff since the time it was fractured and, effectively, relieved. Nevertheless, the general stress state can be easily explained by this simple model and finite element calculations by Clark[29] have shown this. This would suggest that the high stress regions below the interface in Figure 37 are probably the result of stratigraphy, although this has not been confirmed.

If one now examines the coring results with respect to the in situ stresses, it appears the stress peak at 50 ft below the interface correlates well with the point of termination of the lower tip of the first fracture. The stress peak at 180 ft correlates well with the point of termination of the second fracture. It appears that the in situ stress state was the predominant factor controlling the overall fracture geometry. The low stress state in the welded tuff may explain why the first fracture propagated so readily into this rock. One would suspect that with the much higher modulus it would require significantly higher pressures than in the ash-fall tuffs to open a fracture to the necessary widths for injecting grout, even with the natural fracture system. Perhaps the much lower stress state compensates for this. The end result appears to be that in an experiment to test fracture behavior at a geo-

logic interface, the in situ stresses had a much more significant effect than the material property differences.

DISCUSSION

The principal objective of this experiment was to test fracture behavior at a geologic interface between rock strata of considerably different material properties to determine if similar situations in the field (say, a shale/sandstone interface) would contain a hydraulic fracture by terminating or impeding growth. The entire extent of the fractures at the interface was mined back and it was found that the lower green and black fracture was essentially penny-shaped with a radius varying from 50-100 ft. It propagated upward through the interface into the welded tuff as far as it propagated downward. There was no apparent effect due to the higher modulus layer. The fracture did not extend any farther horizontally in the ash-fall tuff than it did in the welded tuff. It did not appear to change orientation or character as it crossed the interfaces through the transition zone into the welded tuff. The only observed differences were somewhat smaller widths in the welded tuff, as one would expect because of the much higher modulus.

These results do not agree with models of fracture behavior at an interface. They are, however, consistent with laboratory experiments which also show that fractures will cross a material property interface.[10,12,13,14] The problem apparently lies in modeling the behavior at the interface using only the stress intensity factor, K, at the tip of the crack for the failure criterion. The concept of K as the strength of the square-root singularity in stress at the crack tip was developed for a crack in a homogeneous body. It is not clear how to extend this concept to the bimaterial interface. Although K may go to zero as the interface is approached, the entire nature and physical meaning of the singularity changes and other singularities now dominate fracture behavior. This should be apparent by observing the stresses. Although

K goes to zero as the interface is approached, the stresses remain infinite and it is, after all, stresses which break the rock. One possible method of avoiding this problem is to use a fracture criterion based on average stress in some region around the crack tip as discussed by Schmidt.[26] Such a criterion would say that fracture growth would occur when the crack tip stress averaged over a meaningful distance reaches a critical value. The critical value would be some applicable strength property of the rock. The meaningful distance could possibly be set using the microcrack model suggested by Schmidt.[26] An average stress calculated in such a way would be directly proportional to the stress intensity factor in a single material. Near a material interface, however, it would incorporate the contributions from all stress singularities. Thus, this criterion would continue to function when the stress intensity approach collapses. An attempt was made during this experiment to measure the size of the process zone near the fracture by making thin sections across the fracture; however, no microcrack zone could be observed.

It is interesting that there is no obvious indication in the pressure records that the fracture broke through the interface. However, there were several shut downs which may have obscured any such signs. It should also be noted that the fracturing pressures are so low that the weight of the column of grout or water was sufficient to fracture, although possibly not to break down the formation. The breakdown pressure was about 735 psi in the ash-fall tuff and about 1400 psi in the welded tuff. Hydraulic head was 610 psi with water and about 1000 psi with the grout.

The effect that natural fractures can have on fracture behavior was seen quite clearly in the mineback and coring results of the green and black lower fracture. As often as not, when the induced fractures intersected a natural fracture, the induced one was offset by a distance ranging from an inch to several feet. In many cases several grout-filled

fractures initiated from the natural fracture afterwards. Many of these natural fractures were filled with grout to distances of 10 ft and others showed green or black halos which indicated there was a large water loss into these fracture systems which resulted in some of the dye being carried out. Apparently, the large amount of cement which was needed to propagate all of the induced strands and to fill the many natural fractures, in addition to the high water-loss rate in this region, accounts for the missing volume from the green and black fracture.

These results show that fracturing in naturally fractured reservoirs is probably considerably less efficient (more leakoff) than in non-fractured reservoirs. It suggests that there are many pitfalls which may hinder treatment of reservoirs such as the Devonian shales or other highly fractured systems. With large treatments there may be many offsets of the hydraulic fracture due to oblique natural fracture systems which may induce several parallel strands. Not only does this pose a problem for fluid loss and resultant fracture length, but proppant transport may be severly restricted by reduced width (if there are several strands) and sharp corners. As a rule, one should expect lower productivity increases as a result of fracture treatments in such formations.

The effects of the in situ stresses can be seen in many aspects of the fracture behavior. For example, the change in dip of the fracture on the NE tip is undoubtedly a reflection of the change in orientation of the minimum principal in situ stress in the region. Except for this area, the fracture is essentially vertical. The slight changes in strike of the fracture may be a result of the fracture following a path along the minimum in the minimum principal stress.

Apparently the fracture propagated readily into the high modulus welded tuff because of the reduced stress state in this stratum. In general, one would expect that it would be more difficult fracturing in a high modulus material because the reduced fracture width would cause large pressure drops in the fracture, resulting in much higher fracturing

pressures. From this argument alone, the fracture should prefer to remain in the much lower modulus ash-fall tuff. However, the much reduced stress state in the welded tuff apparently compensates for this and possibly even results in a lower fracturing pressure in the welded tuff than in the ash-fall tuff.

The in situ stresses also appear to be responsible for the resultant height of the green and black fracture, rather than modulus variations at an interface as originally anticipated. The lower fracture, which was initiated in the ash-fall tuff below the interface, propagated down to a high stress region (300 psi greater) about 50 ft below the interface and not much below. Upwards, it propagated into the low-stress, welded-tuff layer but did not propagate above into the higher stress ash-fall tuff.

The importance of the in situ stress in controlling fracture azimuth and overall geometry has critical implications for fracturing technology. Vertical fracture propagation out of zone (containment) is probably principally controlled by the in situ stress differences between the adjacent layers. Knowledge of the stress difference and practical criteria for use in design calculations should be of utmost interest for realistic design of fracture treatments. Development of in situ stress measurement tools and predictive ability should be a prime area of research effort. The effect of horizontal variations in in situ stress is less obvious but significant changes, as may occur across faults, could terminate lateral extension or reorient the azimuth.

The width appeared to be close to that predicted by design codes. Maximum width of the lower fracture was about 0.4 in near the borehole. It appears that the fracture may have held most of its propagation width as it was designed to do with the low-water-loss cement mixture. Most of the observed variation in width occurs at the tip. On the average, the width throughout the center of fracture is constant, although many

local variations in width occur. Except for these local variations, the width distribution appears to be similar to an elliptic one.

The upper blue or gray fracture is much more difficult to understand. This fracture initiated alongside the first fracture and in many locations propagated along with it. However, for the most part the second fracture propagated downward far below the first one. Very little of the gray grout was found in the welded tuff, which is surprising because the other fracture was found all through this region. This may be due in part to the first fracture, which had previously propagated into this region, filling all the near-wellbore natural fractures as well as initiating many small strands itself. Thus, all the easy fracturing paths had already been cemented closed. Further opening of these fractures in the very high modulus tuffs may have required very high pressures, whereas propagation downward into the low-modulus, moderately-stressed ash-fall tuff may have been the path of least resistance. Essentially, this fracture also had only one wing - on the SW side of the borehole. The results from this fracture were not used for any of the conclusions about fracture behavior due to material property interfaces and in situ stress differences because of these complications, particularly the effect of the first fracture.

CONCLUSIONS

Mineback experiments have been shown to be a valuable technique for investigating hydraulic fracture behavior. It is the only experimentation technique now available for studying fracture behavior with respect to detailed knowledge of reservoir rock properties, geologic conditions (fractures, stratigraphy, etc.) and in situ stresses as well as treatment parameters such as pressure and flow rate. These experiments are conducted in an in situ environment so that there are no size or boundary effects, large scale geologic factors such as fracture systems are effective, and the rock is under in situ conditions.

The results of these fracture experiments conducted in ash-fall and welded tuff formations near a geologic, material-property interface show that high modulus rock layers bounding a lower modulus fracture interval will not prevent fractures from penetrating the interface. In this case, the bounding welded tuff formation had a factor of 5 to 15 higher modulus than the ash-fall tuff, yet the fracture which initiated below the interface in the ash-fall tuff readily propagated across the interface. This is in direct disagreement with present fracture mechanics analyses which predict containment under these conditions. The discrepancy is apparently due to the use of the stress-intensity factor failure criterion which does not hold at a bimaterial interface. The use of an average stress condition instead is suggested. The average stress does not go to zero as the interace is approached and, hence, propagation through the interface would be predicted, although this may be dependent upon other conditions.

The in situ stresses were found to directly control the behavior and geometry of the fracture created in the ash-fall tuff. Results of the minifracs indicate that the minimum principal in situ stress has distinct variability of magnitude, in effect showing "highs and lows" over short distances. Apparently, the fracture responded to these variations by not only propagating perpendicular to the minimum principal stress but also propagating along an irregular path following the "lows" or along the minimum in the minimum principal stress. A region of 300 psi greater in situ stress also terminated the downward growth of the fracture at a point about 50 ft below the interface. The complete propagation of the fracture into the much higher modulus welded tuff is attributed to the much lower stress state found in that stratum compared to the ash-fall tuff. Thus, the in situ stresses appear to have dominated every aspect of fracture growth.

The widths observed in the mineback and exploratory coring are consistent with those predicted by fracture design codes. The overall

width distribution is approximately elliptical with the thickness tapering rapidly at the tips.

Natural fracture systems in the welded tuff had an important effect on the overall fracture behavior. These systems absorbed a large volume of cement, which resulted in many fracture strands propagating parallel to each other at the same time. They were also effective in offsetting the induced fracture a large percentage of the time. The ability to account for only half of the injected volume is attributed in large part to the effect of the natural fracture system.

The upper fracture, which was initiated in the welded tuff, produced few useful results because it initiated and propagated alongside the lower fracture, which had been created at a much earlier time.

ACKNOWLEDGEMENTS

The authors appreciate the efforts of Lynn D. Tyler in the early stages of this experiment and Bob Steanson of Dowell in the design and conduct of this experiment. Many thanks are given to R. J. Dye, R. T. Laws, C. D. Northam, D. South, many other Sandia personnel, M. O'Brien and the skilled mining crew who conducted these tests, evaluations and mining operations in G tunnel. This project is supported by the Office of Oil, Gas, and Shale Technology, United States Department of Energy.

REFERENCES

1. Tyler, L. D. and Vollendorf, W. C., "Physical Observations and Mapping of Cracks Resulting from Hydraulic Fracturing In Situ Stress Measurements," SPE 5542, Dallas, TX, Sept. 28 - Oct. 1, 1975.

2. Tyler, L. D., Vollendorf, W. C., and Northrop, D. A., "In Situ Examination of Hydraulic Fractures," presented at Third ERDA Symposium for Enhanced Oil and Gas Recovery and Improved Drilling Methods, Tulsa, OK, Aug. 30 - Sept. 1, 1977.

3. Warpinski, N. R., Tyler, L. D., Vollendorf, W. C., and Northrop, D. A., "Direct observation of a Sand-Propped Hydraulic Fracture," Sandia National Laboratories Report, in printing.

4. Smith, C. W., Bass, R. C. and Tyler, L. D., "Puff 'n Tuff, A residual Stress Gas Fracturing Experiment," presented at 19th U.S. National Symposium in Rock Mechanics, May 1-3, 1978.

5. Warpinski, N. R., Schmidt, R. A., Northrop, D. A., and Tyler, L. D., "Hydraulic Fracture Behavior at a Geologic Formation Interface: Premineback Report," Sandia Laboratories Report, in preparation.

6. Warpinski, N. R., Northrop, D. A., and Schmidt, R. A., "Direct Observation of Hydraulic Fractures: Behavior at a Formation Interface," Sandia Laboratories Report, SAND78-1935, October 1978.

7. Randolph, P. L., "Massive Stimulation Effort May Double U.S. Gas Supply," World Oil, Oct. 1974, p. 132.

8. Elkins, L. E., "The Role of Massive Hydraulic Fracturing in Exploiting Very Tight Gas Deposits," and Randolph, P. L., "Natural Gas Production from a Tight Sandstone Reservoir in the Green River Basin of Southwestern Wyoming," Natural Gas from Unconventional Sources, National Academy of Sciences, FE-2271-1, 1976.

9. Howard, G. C. and Fast, C. R., Hydraulic Fracturing, Society of Petroleum Engineers of AIME Monograph Series, 1970, Dallas, TX.

10. Daneshy, A. A., "Hydraulic Fracture Propagation in Layered Formations," Soc. Petroleum Engineers Journal, Feb. 1978, p. 33-41.

11. Elder, C. H., "Effects of Hydraulic Stimulation on Coalbeds and Associated Strata," R.I. 8260, U.S. Bureau of Mines, 1977.

12. Teufel, L. W., "An Experimental Study of Hydraulic Fracture Propagation in Layered Rock," Ph.D. Dissertation, Texas A&M University, Aug. 1979.

13. Hanson, M. E., Anderson, G. D., Schaffer, R. J., Hearst, J. R., Haimson, B. and Cleary, M. P., "LLL Gas Stimulation Program, Quarterly Progress Report, April through June 1978," Lawrence Livermore Laboratory Report UCRL - 50036-78-2, July 26, 1978.

14. Hanson, M. E., Anderson, G. D., Shaffer, R. J., Emerson, D. O., Heard, H. C., and Haimson, B. C., "Theoretical and Experimental Research on Hydraulic Fracturing," Proceedings, Fourth Annual DOE Symposium on Enhanced Oil and Gas Recovery & Improved Drilling Methods, Aug. 29-31, 1978, Tulsa, OK.

15. Simonson, E. R., Abou-Sayed, A. S. and Clifton, R. J., "Containment of Massive Hydraulic Fractures," Society of Petroleum Engineers Journal, February, 1978, p 27-32.

16. Cleary, M. P., "Rate and Structure Sensitivity in Hydraulic Fracturing of Fluid-Saturated Porous Formations," Proceedings, 20th U. S. Symposium on Rock Mechanics, June 4-6, 1978, Austin, TX, p 127-142.

17. Brechtel, C. E., Abou-Sayed, D. S., and Jones, A. H., "Fracture Containment Analysis Conducted on the Benson Pay Zone in Columbia Well 20538-T," Proceedings, Second Eastern Gas Shales Symposium, October 1978, Morgantown, West Virginia.

18. Jones, A. H., Abou-Sayed, A. S., and Rogers, L. A., "Rock Mechanics Aspects of MHF Design in Eastern Devonian Shale Gas Reservoirs," Proceedings, Third ERDA Symposium on Enhanced Oil, Gas Recovery and Improved Drilling Methods, August 30-31, Sept. 1, 1977, Tulsa, OK.

19. Hanson, M. E., Anderson, G. D., Shaffer, R. J., Emerson, D. O., Swift, R. P., O'Banion, K., Cleary, M. P., Haimson, B. Knutson, C. F., and Broadman, C. R., "LLL Gas Stimulation Program, Quarterly Progress Report, July through September, 1978," Lawrence Livermore Laboratory Report WCRL-50026-78-3, November 6, 1978.

20. Cook, T. S., and Erdogan, F., "Stresses in Bonded Materials with a Crack Perpendicular to the Interface," Inter. J. of Eng. Sci., Vol. 10, pp. 677-697, 1973.

21. Erdogan, F., and Biricikoglu, V., "Two Bonded Half Planes with a Crack Going Through the Interface," Inter. J. Of Eng. Sci., Vol. 11, pp. 745-766, 1973.

22. Atkinson, C., "On the Stress Intensity Factors Associated with Cracks Interacting with an Interface Between Two Elastic Media," Inter. J. of Eng. Sci., Vol. 13, pp. 489-504, Sept. 1972.

23. Leverenz, R. K., "A Finite Element Stress Analysis of a Crack in a Bi-Material Plate," Inter. J. of Fracture Mechanics, Vol. 8, No. 3, pp. 311-324, Sept. 1972.

24. Bogy, D. B., "On the Plane Elastostatic Problem of a Loaded Crack Terminating at a Material Interface," J. of Applied Mechanics, Vol. 38, pp. 911-918, August 1975.

25. Rogers, L. A., Simonson, E. R., Abou-Sayed, A. S., and Jones A. H., "Massive Hydraulic Fracture Containment Analysis Utilizing Rock Mechanics Considerations," Procedures of the Massive Hydraulic Fracturing Symposium, University of Oklahoma, Norman, OK, February 28 - March 1, 1977.

26. Schmidt, R. A., "A Microcrack Model and Its Significance to Hydraulic Fracturing and Fracture Toughness Testing," 21st U. S. Symposium on Rock Mechanics, Rolla, Missouri, 1980.

27. Geertsma, J. and de Klerk, F., "A Rapid Method of Predicting Width and Extent of Hydraulically Induced Fractures," J of Petroleum Technology, December 1969, p. 1571.

28. Northrop, D. A. and Schuster, C. L., "Enhanced Gas Recovery Program Third Annual Report, Oct. 1977 - Sept. 1978," Sandia National Laboratories Repot, SAND79-0056, March 1979.

29. Clark, J. A., Personal Communication.

DISTRIBUTION:

TIC - 4500 - UC-92a (206 copies)

M. R. Adams
Office of the Deputy Assistant
Secretary for Oil, Gas and
Shale Technology
U. S. Department of Energy
Mail Stop D-107
Washington, DC 20545

B. G. DiBona
Office of the Deputy Assistant
Secretary for Oil, Gas and
Shale Technology
U. S. Department of Energy
Mail Stop D-107
Washington, DC 20545

P. R. Wieber
Office of the Deputy Assistant
Secretary for Oil, Gas and
Shale Technology
U. S. Department of Energy
Mail Stop D-107
Washington, DC 20545

J. B. Smith
Office of the Deputy Assistant
Secretary for Oil, Gas and
Shale Technology
U. S. Department of Energy
Mail Stop D-107
Washington, DC 20545

C. H. Atkinson
U. S. Department of Energy
Nevada Operations Office
P. O. Box 14100
Las Vegas, NV 89114

H. C. Johnson
U. S. Department of Energy
Bartlesville Energy Technology
Center
Bartlesville, OK 74003

D. C. Ward
U. S. Department of Energy
Bartlesville Energy Technology
Center
Bartlesville, OK 74003

H. B. Carroll
U. S. Department of Energy
Bartlesville Energy Technology
Center
Bartlesville, OK 74003

A. B. Crawley
U. S. Department of Energy
Bartlesville Energy Technology
Center
Bartlesville, OK 74003

A. A. Pitrolo
U. S. Department of Energy
Morgantown Energy Technology Center
Box 880, Collins Ferry Road
Morgantown, WV 26505

C. D. Locke
U. S. Department of Energy
Morgantown Energy Technology Center
Box 880, Collins Ferry Road
Morgantown, WV 26505

A. E. Hunt
U. S. Department of Energy
Morgantown Energy Technology Center
Box 880, Collins Ferry Road
Morgantown, WV 26505

C. A. Komar
U. S. Department of Energy
Morgantown Energy Technology Center
Box 880, Collins Ferry Road
Morgantown, WV 26505

R. D. Manilla
U. S. Department of Energy
Morgantown Energy Technology Center
Box 880, Collins Ferry Road
Morgantown, WV 26505

R. L. Mann
CER Corporation
P. O. Box 15090
Las Vegas, NV 89114

J. C. Sharer
Gas Research Institute
10 West 35th Street
Chicago, IL 60616

R. L. Huggins
Amoco Production Co.
Research Department
P. O. Box 591
Tulsa, OK 74120

R. W. Veatch
Amoco Production Co.
Research Department
P. O. Box 591
Tulsa, OK 74102

DISTRIBUTION (cont)

M. B. Smith
Amoco Production Co.
Research Department
P. O. Box 591
Tulsa, OK 74102

L. F. Elkins
Sohio Petroleum Co.
50 Tenn Place, Suite 1100
Oklahoma City, OK 73118

T. W. Muecke
Exxon Production Research Co.
P. O. Box 2189
Houston, TX 77001

J. L. Gidley
Exxon Production Research Co.
P. O. Box 2189
Houston, TX 77001

F. G. Martin
Altlantic Richfield Company
P. O. Box 2819
Dallas, TX 75221

R. J. Saucier
Shell Development Co.
P. O. Box 481
Houston, TX 77001

C. Murphy
Mobil Research & Development Corp.
P. O. Box 900
Dallas, TX 75221

J. L. Fitch
Mobil Research & Development Corp.
P. O. Box 900
Dallas, TX 75221

L. Medlin
Mobil Research & Development Corp.
P. O. Box 900
Dallas, TX 75221

A. B. Waters
Halliburton Services Research
Center
P. O. Box 1431
Duncan, OK 73533

A. A. Daneshy
Halliburton Services
Reseach Center
P. O. Box 1431
Duncan, OK 73533

R. Steanson
Dowell
P. O. Box 21
Tulsa, OK 74102

R. P. Trump
Gulf Research and Development Co.
P. O. Drawer 2038
Pittsburgh, PA 15230

B. B. McGlothlin
Gulf Research and Development Co.
P. O. Drawer 2038
Pittsburgh, PA 15230

M. E. Hanson
L-200
Lawrence Livermore Laboratory
Livermore, CA 94550

N. Vanderborgh
G-7
Los Alamos National Laboratory
Los Alamos, NM 87545

H. C. Walther
Conoco
Production Research Divisonm
Ponca City, OK 74601

Robert Forrest
Columbia Gas System Service Corp.
1600 Dublin Road
Columbus, OH 43215

M. D. Wood
770 Welch Road, #335
Palo Alto, CA 94304

P. L. Randolph
Institute of Gas Technology
3424 S. State Street
Chicago, IL 60616

Western Gas Sands Project Library
CER Corporation
P. O. Box 15090
Las Vegas, NV 89114

USGS Special Projects Branch
P. O. Box 25425
Denver Federal Center
Denver, CO 80225
Attn: R. Carroll
W. Ellis

USGS Special Projects Branch
Core Library
P. O. Box 45
Mercury, NV 89023

DISTRIBUTION (Cont)

Fenix & Scisson, Inc.
P. O. Box 498
Mercury, NV 89023
Attn: G. Bruesch
D. Townsend
M. O'Brien

Defense Nuclear Agency
P. O. Box 208
Mercury, NV 89203
Attn: J. LaComb

1 M. Sparks
1000 G. A. Fowler
1100 C. D. Broyles
1110 J. D. Plimpton
Attn: C. R. Mehl, 1112
1112 C. W. Smith
1130 H. E. Viney
Attn: R. D. Statler, 1133
1131 B. G. Edwards
1131 R. J. Dye
1133 W. C. Vollendorf (10)
4500 E. H. Beckner
4537 L. D. Tyler
4700 J. H. Scott
4740 R. K. Traeger
Attn: B. Granoff, 4746
P. J. Hommert, 4747
B. E. Bader, 4748
4750 V. L. Dugan
Attn: B. W. Marshall, 4755
4751 J. R. Tillerson
4752 H. M. Dodd
4753 D. A. Northrop (25)
4753 N. R. Warpinski (25)
4753 S. J. Finley (5)
4754 A. F. Veneruso
5500 O. E. Jones
5520 T. B. Lane
5530 W. Herrmann
Attn: B. M. Butcher, 5532
5541 W. C. Luth
8214 M. A. Pound
3141 L. J. Erickson (5)
3151 W. L. Garner (3)
3154-3C. Dalin
For DOE/TIC (Unlimited Release)